TRACE3D

Empowering Integrated Electromechanical 3D Printing

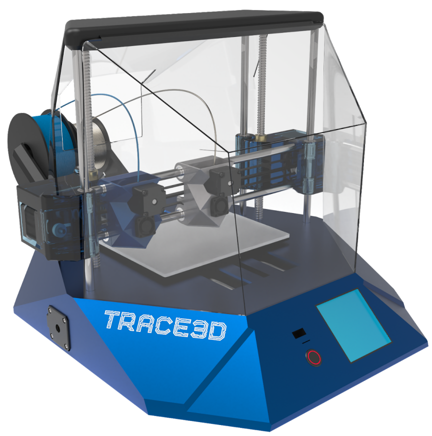

Final Project Report for MEAM 445/446

September 2020 - April 2021 | Submission Date: May 7th, 2021

Jared Rogers
MEAM M&T '21 | MSE '22
jarederogers@gmail.com

Kevin Chazotte
MEAM '21 | ROBO '21
kevinchazotte@aol.com

John Berg
MEAM '21
bergjohn5@gmail.com

Owen Ford
MEAM '21
owen.ford@outlook.com

Aviva Hurvitz
MEAM '21 | IPD '22
ahurvi@gmail.com

Faculty Advisor

Mark Yim
Asa Whitney Professor of Mechanical Engineering
yim@seas.upenn.edu

Abstract

Hobbyist and professional makers desire complete design and creative freedom while prototyping. Most of their projects involve both mechanical and electrical components, especially highly functional electronics such as printed circuit boards (PCBs). Integrating conventional mechanical systems with PCBs often leads to prototypes that are built suboptimally, are time-intensive to assemble, and are expensive. Integrated electromechanical 3D printing, which combines 3D printing with PCB design capabilities, is one solution under development for reducing these limitations. However, the high cost of proposed solutions significantly limits adoption by makers and other cost-constrained users.

Team Trace3D designed and manufactured a proof-of-concept electromechanical 3D printer that uses off-the-shelf materials to create physical prototypes that integrate insulative structural components and conductive pathways in three dimensions. This frees designers from the constraints of traditional flat PCBs, leading to increased design freedom and simplified product development cycles.

A one-dimensional gantry was initially used to test deposition mechanisms, collect data, and validate the team's modeling efforts. Utilizing a heavily retrofitted Ender 3 Pro, Trace3D demonstrated proof-of-concept by extruding a conductive material, in Trace3D's case solder wire, onto a plastic coupon in three dimensions. The measured resistance must be under 0.25 Ω for a representative trace and the full print must take less than 15 minutes to post-process. Anticipated fixed cost of the system is under \$750 with a material cost of under \$65/kg.

Table of Contents

Introduction **4**
Project Inspiration 4
Statement of Need 4
Possible Applications 5
Robotics 5
University Projects 5
Quadcopters 5
Existing Solutions 5
Extension of the Solution Space 6
Social Impacts of the Solution 8

Characteristics and Constraints **9**
Stakeholder Interactions 9
Stakeholder-Driven Solution Characteristics 9
Design Impact of Engineering Standards 11
Additive Manufacturing Standards 11
Electronics Standards 12
Solder Alloy Standards 12

Design, Engineering, and Realization **13**
Downselection 13
Project Direction 13
Conductive Material Selection 14
Insulative Material Selection 14
Hotend Selection 15
Extruder Selection 16
Nozzle Selection 17
Quantitative Analysis - Solder Deposition 17
Solder Deposition and Flow Regime 17
Hotend Temperature and Feed Rate 19
Quantitative Analysis - Conductive/Insulative Material Heat Transfer 21
Cooling of Solder Traces 21
PLA Heat Transfer 22
1D Gantry Validation Testing 23

Final System Form **25**
3D Implementation Gantry 25
G-Code Generation 26
Octoprint 26
MATLAB 26
Solder Bridging 27
Java Slicer 28
Parameter Tuning 29
Future Iterations 30
System Performance **31**
Material Exploration 31
Test Print Totem 32
Achieving Stakeholder Benchmarks 33
Conclusions and Future Work **34**
Statement of Roles **35**
John Berg 35
Kevin Chazotte 35
Owen Ford 35
Aviva Hurvitz 35
Jared Rogers 35
Acknowledgements **36**
References **37**
Appendix **41**
Competitive Landscape 2x2 Comparison 41
Quadcopter Development 42
Resistivity of Solder Traces 43
Solder Deposition 44
Circuit Diagram & Soldered Perf Boards 45
Experimental Data from 1D Test Gantry Testing 46
Drone Totem Iterations 47
Pictures of Successful Drone Totem Print 47

1. Introduction

1.1. Project Inspiration

Throughout our time at the University of Pennsylvania, our team has been intimately exposed to numerous electromechanical systems. We have designed enclosures for scientific measuring equipment, packaged high voltage circuits for the Penn Electric Racing team, built robots for mechatronics class, and breadboarded for a plethora of engineering lab projects. We all have felt similar pain points in these projects: electromechanical integration significantly inhibited our design freedom. The inspiration for this project resulted from musings over whether this pain point was felt by others.

Printed Circuit Board (PCB) fabrication and Fused Deposition Modeling (FDM) 3D printing are both well-understood and relatively cheap manufacturing methods. However, despite the improved design freedom they individually offer over traditional methods, electromechanical integration is still very limiting. FDM 3D printed parts can be geometrically complex but are limited in that they cannot easily incorporate electronic components without specially designed features. PCBs are ubiquitous in the electronics industry but are relegated to only flat profiles. Consultation with dozens of stakeholders affirmed that reducing the limitations that PCBs, electronics, and wire-management impose on mechanical design was indeed a problem worth solving.

1.2. Statement of Need

The casual hobbyist maker desires complete design freedom for high quality, creative one-off prototyping. University researchers and students frequently require cheap, easy to use, and unique setups for projects and experimentation. Most of these applications involve both mechanical and electrical components, namely PCBs and other functional electronic components. While the process of fabricating PCBs is inexpensive, producing systems that integrate conventional mechanical systems with PCBs often leads to prototypes that are built suboptimally, are time-intensive to assemble, and are expensive - ultimately limiting design freedom.

A system that reduces the limitations that mechanical components place on electrical devices would open doors to new design spaces. Electromechanical 3D printing is one solution that is currently under development since combining the capabilities of 3D printing with PCB design could drastically increase design freedom. Imagine quadcopters with fully hidden electronics, robotics with degrees of freedom not limited by wire length, and sensors with built-in mechanical strength. However, proposed solutions have not yet hit the consumer market and the cost of proposed systems limit adoption by makers and other cost-constrained users. Trace3D is a proof-of-concept electromechanical 3D printer that uses off-the-shelf materials to create physical prototypes that integrate insulative structural components and conductive pathways in three dimensions. With Trace3D, designers would no longer be constrained by flat PCBs, and instead mechanical and electrical elements can be perfectly integrated into compact product footprints. The value propositions of such a solution are increased design freedom, more creativity, simplified development cycles, and aesthetic and functional improvements for electromechanical systems.

1.3. Possible Applications

Integrated electromechanical 3D printing has many exciting applications for which increased design freedom for prototyping and manufacturing would be desirable.

Robotics

One substantial need in the maker community is an easier and more efficient way to 3D print robotic components. Robotics have become especially popular among younger maker communities, with projects ranging from miniature soccer-playing robots to electromechanical prosthetics for personal injuries. By printing electronic components into the body of the project, the tendency for external wires to restrict degrees of freedom and range of motion can be markedly reduced.

University Projects

At the university level, such capabilities would be very beneficial for engineering design and project-based courses as well as for testing setup enclosures. Trace3D could substantially increase the aesthetic and functional quality of projects in research and classes. Instead of relying on hastily thrown together breadboards or perfboards, students and researchers could integrate their wiring needs directly into CAD models to output fully electromechanical devices. This could further result in decreased footprints and build volumes.

Quadcopters

One other specific application for Trace3D could be in the design and manufacturing of quadcopters, which are a particularly coveted DIY project for makers. A regular quadcopter will usually have messy wires and heavy fasteners holding its electronic components together, but with Trace3D and its integrated trace capabilities, the quadcopter becomes significantly simpler, as seen in *Figure 1*.

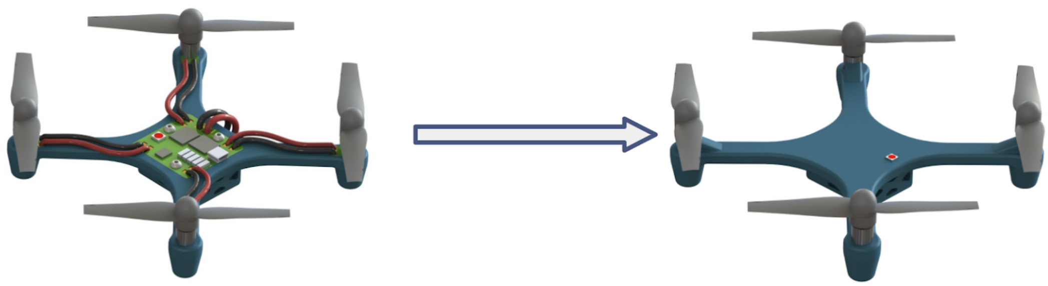

Figure 1: Regular Quadcopter (left) vs. Trace3D Quadcopter (right)

Integrating circuits into the mechanical structure can potentially lead to a cleaner aesthetic, better aerodynamics, and lower weight and hence better battery life.

1.4. Existing Solutions

While desktop 2D PCB printers and industrial-grade 3D electromechanical printers exist, there are currently no affordable options that use readily available materials for fast prototyping. *Table 1* shows where these competing products fall on four metrics: dimensionality, price, build time, and market.

Table 1: Existing Competition for Electromechanical Printing [1, 2, 3, 4, 5, 6, 7, 8]

Name	2D or 3D	Price	Speed	Market
Breadboarding	2D	Varies	Hand Speed	Prototyping
Traditional PCB Design	2D	Varies	Lead Time Based	Industrial
Botfactory SV2	2D	$4,999	50 in/min	Prototyping
Voltera V-One	2D	$4,200	20 in/min	Prototyping
Zippy Robotics Prometheus	2D	$2,992	150 in/min	Prototyping
Bantam Tools PCB Mill	2D	$3,300	100 in/min	Prototyping
Neotech AMT PJ15X	3D	$65,000	230 in/min**	R&D
Neotech AMT PJ15X	3D	$250,000	2360 in/min**	Industrial
Optomec Aerosol Jet	3D	$500,000**	225 in/min**	Industrial
ND DragonFly LDM	3D	$300,000**	3-5s/layer**	Industrial
Voxel8 Developer's Kit*	3D	$8,999	120 in/min**	Prototyping

* Discontinued

** Estimates from conference materials, industry research, or video analysis

The closest option to Trace3D's market niche is the Voxel8 Developer's Kit, which is indeed a 3D integrated electromechanical printer for prototyping; however, the Voxel8 was discontinued from production in 2016 and the company has since pivoted to only 3D printing shoe uppers. While Voxel8 still believes in the future potential of the electromechanical 3D printing market, they pivoted to athletic footwear uppers due to lucrative partnerships offering greater returns in the short-run [9]. Furthermore, the Voxel8 Developer's Kit cost $8,999 when it was available to purchase, comfortably positioning it as a higher cost option in the market. Voxel8 also used a proprietary, expensive silver colloidal paste which costs $1000/kg [10], placing it further out of reach for Trace 3D's target market.

While the Neotech AMT PJ15X, Neotech AMT 45XG3, Optomec Aerosol Jet, and Nano Dimension DragonFly LDM are also electromechanical printers capable of operating in the third dimension, they are all expensive and primarily intended for scalable industrial applications. None of these are accessible, or necessary, purchases for the average maker or university engineering department.

Other alternative solutions to Trace3D include traditional breadboarding and PCB designing. Despite their ubiquity, these are the root causes of the pain points identified by Trace3D's stakeholders in many cases. Breadboarding is messy, prone to disconnections, and not scalable, and the flat PCB profile limits all electronic elements to be oriented in orthogonal directions. Diametrical comparisons of this solution space on 2x2 charts can be found in **Appendix A1**.

1.5. Extension of the Solution Space

What primarily differentiates Trace3D from these traditional methods is the significantly simplified workflow involved. For purposes of demonstration, take the quadcopter example from Section 1.3. A traditional development cycle for a quadcopter is represented in *Figure 2*.

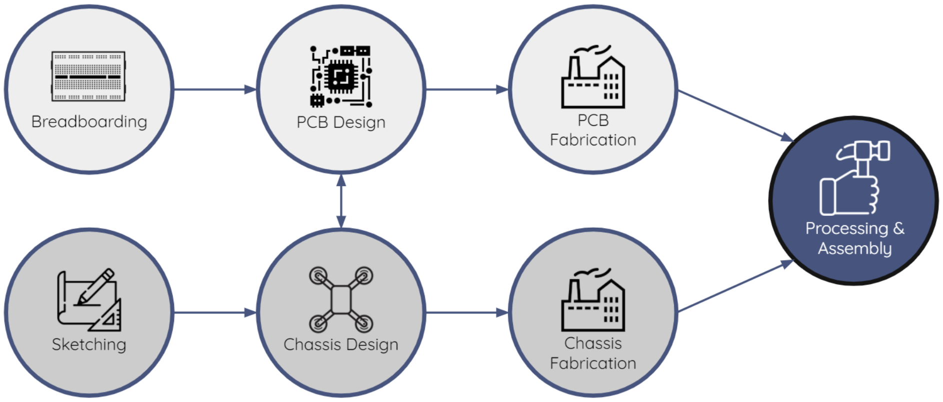

Figure 2: Traditional Quadcopter Development Cycle

Evidently, this traditional quadcopter design cycle involves nearly parallel mechanical and electrical development streams. Breadboarding leads to PCB layout and eventually PCB fabrication while mechanical sketching leads to design of the chassis in CAD and eventually chassis fabrication. However, significant communication must take place between mechanical and electrical development teams during the design stages to ensure proper fits and tolerancing for all components. More collaboration is then necessary at the processing and assembly stage of development.

With Trace3D, development cycles can be greatly simplified, as seen in *Figure 3*.

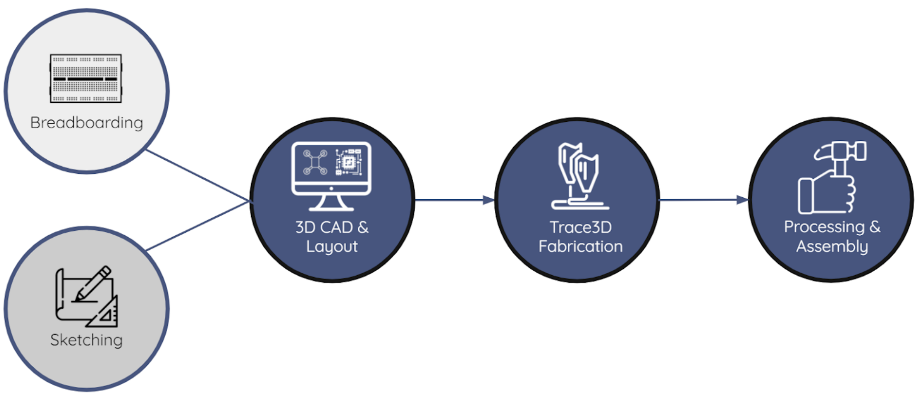

Figure 3: Trace3D Quadcopter Development Cycle

Breadboarding and sketching still occur separately in this workflow, but in large part, 3D CAD and electronic layout are completed together, followed by Trace3D integrated fabrication and any remaining processing and ancillary assembly steps. Although communication between mechanical and electrical teams, if needed, will certainly still be necessary, the enhanced collaboration would lead to a simpler workflow overall. Visualizations of this drone assembly process can be found in **Appendix A2**.

1.6. Social Impacts of the Solution

Trace3D will lead to democratized access to high quality electromechanical manufacturing equipment, potentially leading to many positive social impacts. For example, there is a huge opportunity to revolutionize how design and electronics are taught at both the high school and university levels. The need for more accessible, cheaper, and easier to use tools in STEM education is a major social impact cause that Trace3D seeks to address. Even over just the past five years, elite high schools across the country have promoted STEM education by constructing maker spaces that allow students early access to design and engineering education [11]. There is a major push in the United States to promote STEM education in schools at an early age. Trace3D could work with these schools and other community-based organizations to serve as both a resource and a partner—to provide the tools, materials, and expertise that empower students to become makers. By giving access to Trace3D printers at a discounted cost—along with educational resources and curriculum planning guides to teach the fundamentals of design, circuitry, electronics, and fabrication—we can empower teachers and school faculty to promote and encourage STEM education for students across the country.

Trace3D is also targeted for makerspaces in order to make electromechanical design and manufacturing more accessible to the global community. Makerspaces are physical spaces for open collaboration between people who have access to resources, knowledge, professional connections, and tools, and those who need them for developing and prototyping projects to create products or services. These spaces are key drivers of community and city growth and development. According to statistics cited in a 2016 National League of Cities report entitled "How Cities Can Grow: the Maker Movement", an estimated 135 million U.S. adults are "makers," 26% of U.S. cities have makerspaces, and there are an estimated 2,000 makerspaces around the world [12]. Makerspaces connect people with each other to provide support, share lessons learned, and provide tools for users to develop new creations. Trace3D is yet another tool in the arsenal of resources that makers can use to promote creativity, collaboration, innovation, and social impact at their makerspaces and in their communities at large.

Currently, most electronic equipment is shipped overseas from China [13], creating a large environmental impact. Most printed circuits boards are produced in the Asia-Pacific region, representing more than 90% of global PCB production. China meets about 50% of global PCB and PCBA demand on its own [13]. Over the last five years, China's PCB manufacturing sector grew by 8.4% to reach $95 billion [14]. While the cost to produce and ship PCBs from China to the U.S. is low, the environmental impact is much larger. Scientists calculated that in 2015, US–China trade accounted for 2.5% of global carbon-dioxide emissions due to the extensive shipping involved. This number is expected to increase by 250% by 2050 if no action is taken [15]. Trace3D can reduce the need to buy printed circuit boards internationally by enabling people to instead design and create their own. This could in turn significantly reduce the environmental impact of PCB shipping and improve public health and welfare.

2. Characteristics and Constraints

2.1. Stakeholder Interactions

Trace3D's interactions with stakeholders are divided into three primary categories: industry practitioners, university professors, and maker archetypes. One industry practitioner interviewed is the Director of Enterprise Solutions at Dynamism Inc, an industry-leading 3D printing solution provider for business and education. This stakeholder was knowledgeable in 3D printing with metal from his time working at Desktop Metal and remarked that Trace3D would fill a much-needed gap in the market. We further spoke with a startup founder who is currently designing hardware and software for a laboratory setting. Their hardware is driven by several custom PCBs contained within 3D printed enclosures. A fully integrated electromechanical printer, with high speed, resolution, and build volume would have been of interest to them during their past development cycle.

We also interviewed a diverse set of Penn professors with domains of expertise including materials science, manufacturing, PCB design, product design, and maker spaces. Many of these professors affirmed the usefulness of this idea, and some even suggested additional useful applications. One professor indicated that 3D printing PCBs could allow for several complex design variations to be produced concurrently, saving significant development time. Two instructors who own maker equipment themselves, including several 3D printers each, specified that they would be potentially interested in purchasing and using a refined version of this device. Further insights from these conversations revealed that quality and accuracy should be prioritized over cost and speed for research applications, while the opposite prioritization should be made for student and maker projects.

Further affirmation of this need came from interacting with active members of the maker community. One maker we spoke with often showcases at "Maker Faires" and has an active following on his maker YouTube channel. He explained that makers at the makerspace he uses find it too expensive and time-consuming to fabricate the custom PCBs needed for their projects. Instead, they usually turn to breadboarding or perfboarding. This makes them feel unnecessarily constrained and dissatisfied with a messy, unorganized, and visually unprofessional final product. Another maker we interacted with is the Makerspace Director at a top private school in New York who teaches an introduction to electronics, coding, and rapid prototype fabrication class for high school freshmen. He too expressed avid interest in an electromechanical 3D printer, as it would allow his students to create more aesthetically pleasing and higher quality final projects. Further feedback from makers was gathered from the Additive Manufacturing Subreddit, where we interacted with and received advice and positive feedback from a dozen makers familiar with 3D printing technologies.

2.2. Stakeholder-Driven Solution Characteristics

In service of understanding what solution characteristics are most essential for Trace3D's stakeholders, we distributed a survey that was completed by 91 makers. For purposes of this survey, "maker" is defined as any student, professor, or professional who has hands-on experience with mechanical or electrical systems. 94.5% of respondents have used a 3D printer and 18.7% own one themselves;

additionally, many are also skilled in operating laser cutting and metal fabrication tools. 90.2% of respondents have extensive experience using electronics, including breadboarding, microcontrollers, and PCB design. Most importantly, 80.2% of respondents have either designed or built something with both mechanical and electrical components, such as a drone or robot, test setup, or student project. *Table 2* summarizes issues these makers have encountered with electromechanical design, ordered by relative frequency.

Table 2: Most Popular Electromechanical Design Problems Encountered

Ranking	Issue Encountered	% of Respondents
1	Messy and hard to route wires	75.8%
2	Ugly aesthetics	61.5%
3	Things getting unplugged	59.3%
4	Modifying mechanical design for electronic components	56.0%
5	Understanding how to design electromechanical systems	50.5%
6	Designing mechanical and electrical components separately	44.0%
7	Difficulty designing enclosure for electronics	38.5%
7	Restricted motion or degrees of freedom	38.5%
8	Larger than anticipated resulting build volume	33.0%
9	Heavier than anticipated resulting product	26.4%
10	Optimizing component, chip, or PCB placement	25.3%

In the second half of this survey, respondents read a generalized elevator pitch for Trace3D and then responded to a series of questions assessing their thoughts. Further questions were designed to gauge stakeholder sensitivities to the project design parameters.

85.7% of respondents said that Trace3D would be a useful tool for makers, with an additional 13.2% indicating "maybe." 23.1% of people said they were "very interested" and an additional 53.8% said they were "interested" in the device themselves. The average permissible variable cost per part arrived at between 3.25x and 3.65x the price of a standard FDM 3D printed part, depending on size. Respondents were also asked about the fixed costs they would be willing to pay, as shown in *Table 3*.

Table 3: Payment Sensitivity Matrix Resulting from the Maker Survey

Response	Pay $2000	Pay $1000	Pay $500
Extremely Likely	4.4%	6.6%	28.6%
Likely	5.5%	22.0%	27.5%
Unsure	33.0%	30.8%	15.4%
Somewhat Unlikely	25.3%	12.1%	14.3%
Very Unlikely	31.9%	28.6%	14.3%

Each of the gray blocks represents approximately equal percentages of respondents. As shown, significant sensitivity exists between the $1,000 and $2,000 price values, although much more buy-in is achieved at the $500 price point. Therefore, a target large scale production price of $750 is plausible.

Benchmarking against the Ender 3 Pro FDM printer's standard speed of approximately 100 in/min [16], most makers said they would be okay with an electromechanical printer being significantly slower. 19.8% of respondents answered it could be less than half as fast, 28.6% expect it to take around half as fast, and 40.7% would accept speeds up to three-quarters as fast. A majority of makers, 74.8%, expect less than 15 minutes of necessary post-processing per part. Most respondents also expect printed traces to be as conductive as possible, with a minimum performance equivalent to that of Voxel8's silver colloid resistivity of 50×10^{-8} Ωm [17] and ideally as close to the resistivity of a copper trace as might be found in a traditional printed circuit board. The need for high conductivity was affirmed by many of the other stakeholder interactions outlined above.

After filtering through and analyzing response patterns for outliers, including taking a close look at the sensitivities of those who were most interested in the product, we were able to develop a set of quantitative thresholds that Trace3D must conform to:

1) A **fixed cost of under $750**, derived from stakeholder fixed cost sensitivity analysis.
2) A **material variable cost of under $65/kg**, or 3.25x that for a regular FDM 3D printer [18].
3) A **trace resistance of under 0.25 Ω**. This is derived by non-geometricizing the electrical resistivity of copper for what may be expected from a typical 2.5 inch long PCB trace. Further details on this calculation and derivation are found in **Appendix A3**, but in essence this benchmark allows for maximized conductivity without lost performance based on what the stakeholder survey indicated is important to potential system users.
4) **Exactly 3 build dimensions**, to meet the expectation that Trace3D be a true 3D printer.
5) A **print speed over 50 in/min**, benchmarked off stakeholders' thoughts on the Ender 3 Pro.
6) A **post-processing time of under 15 minutes** per part, defined as any soldering, support removal, or other ancillary processing and assembly necessary.

2.3. Design Impact of Engineering Standards

Several standards drove how this project was conducted, thought about, and implemented. These standards spanned domains including additive manufacturing, printed and general electronics, as well as mechanics and properties of materials. What follows is a brief overview of how these standards impacted system design and performance.

Additive Manufacturing Standards

Designing a 3D printer of any sort involves using a standardized set of terminology to describe its various parts and functions. ASTM 52900 [19] provides a broad set of definitions and principles related to additive manufacturing, and although now withdrawn, ASTM F2792 [20] adds even more definitions that differentiate between 3D printer process categories. ISO/ASTM 52921 [21] defines notation approaches for describing 3D printer coordinate systems, build volumes and bounding boxes, as well as build speed and feed rates. This standard was consulted as key performance metrics for the Trace3D system were determined and validated. Finally, although outside the scope of the project at present, ASTM F3122 [22] is the standard for evaluating mechanical properties of metal materials made via additive manufacturing processes. Ensuring mechanical integrity of the Trace3D conductive prints is a next step for project development and this standard has been bookmarked for that purpose.

Electronics Standards

Since Trace3D aims to 3D print fully functional circuit boards, there are specific standards that govern the requirements for both printed electronics base materials and printed electronics functional conductive materials. IPC-4921A [23], which governs requirements for the base or substrate material, was consulted as insulative material selection occurred. Options for printed electronic base materials are classified based on the base material family, material type, base structure, reinforcement type, and thickness, and the standard indicates that thermoplastic elastomers in general and several types of commonly 3D printable plastics are permissible to use. IPC-4591A [24], which governs requirements for the conductive material, was similarly consulted as conductive material selection occurred to ensure compatibility with industry standards.

Solder Alloy Standards

Since, as will be discussed in Section 3.1 below, solder wire was chosen as the conductive material for Trace3D, standards regarding solder wire and solder alloys were heavily consulted throughout the project. ASTM B32-08 [25] is the standard specification for solder metal and covers expected melting ranges, name designations for how to identify various solder alloys, how to safely test with solder, and how to measure for material resistivity. This standard was further employed in initially determining what type and quantity of flux could be usable for this project; however, as will be explained in Section 5.2, fluxless solder was eventually selected as the material of choice.

The other most impactful standard consulted with regard to solder alloy selection was ANSI/J-STD-006 [26], which sets requirements for electronic grade solder alloys and fluxed and non-fluxed, solid solders for electronic soldering applications. Given that this was the crux of the project, this standard was consulted the most. All electronic grade solder alloys are listed in Appendix A, Table A-1 of this standard; only solder alloys which appeared on this table were selected for further exploration in this project. This standard further enumerated how varying alloying elements in solder alloys impact performance and what some of their most pertinent properties are. For example:

- Bismuth is used to achieve lower soldering temperatures and it wets poorly to metal
- Copper is used to reduce tip degradation of soldering irons, which can be extended to nozzles
- Indium is used for wetting to non-metallic surfaces and lower melting temperatures even more
- Silver is used to increase wettability, reduce thermal stress, and improve strength

As solder alloy selection occurred, these material properties were frequently consulted so that all testing efforts were focused on the candidates most likely to be successful. The best solder alloy that was considered has a datasheet which specifically calls out its compliance with this standard [27].

3. Design, Engineering, and Realization

3.1. Downselection

Project Direction

In its final form, Trace3D will be a completely vertically integrated manufacturing platform for electromechanical systems. This will include insulative substrate and conductive element deposition systems as well as pick and place functionality for embedding electrical components such as resistors, capacitors, and integrated circuits within an enclosure. Given the difficult maintenance associated with such a build, this would, at least initially, be limited to rather simple electrical designs but could be embedded in very complex FDM 3D printer generated shapes. However, with the consistent uncertainty and limited facility access as a result of the COVID-19 pandemic, this project was scoped down substantially to focus on just embedding conductive traces in an insulative matrix. To do this, it was initially hypothesized that a conductive material could be extruded, melted, and shaped onto a plastic wafer using a similar setup to a typical FDM printer.

However, before diving into this design, multiple potential solution spaces were considered to ensure that such a system was indeed the optimal direction for the project. These additional solutions included inkjet printing circuits, flexible PCBs, embedded PCBs, and fragmented PCBs. Inkjet printing circuits involves printing silver nanoparticle ink from a traditional inkjet printer. A flexible PCB contains electronic traces mounted on a flexible plastic substrate. Embedded PCB would involve a 3D printer fabricating one half of the enclosure for a PCB, inserting the PCB manually, and then printing the second half of the enclosure on top. A fragmented PCB would involve breaking a traditional circuit board into parts connected via wires; these parts would then be installed into smaller spaces available within the natural design of the product. These solutions were evaluated along with normal PCBs and electromechanical 3D printing over 5 metrics, as shown in *Table 4*. Of note, this downselection process was preliminary and meant only to guide the initial stakeholder engagement for the project. More detailed, quantitative downselection processes on key system considerations and subsystems are discussed later in this section.

Table 4: Initial Downselection of Ideas Related to Improving Electromechanical Integration

Solution	Geometric Limitation	Time Scale to Manufacture	Time Scale to Assemble	Ease of Assembly	Build Dimensions
Threshold	**Low**	**Hours**	**Minutes**	**Easy**	**3**
Electromechanical 3D Printing	None	Hours	Minutes	Easy	3
InkJet Printing	Low	Hours	Minutes	Easy	2
Flexible PCB	Low	Weeks	Hours	Moderate	3
Embedded PCB	Low	Weeks	Hours	Difficult	2
Fragmented PCB	Moderate	Weeks	Days	Difficult	2/3
Normal PCB	High	Days	Hours	Moderate	2

Better Than Threshold	At Threshold	Deviates Moderately	Non-Starter

These approaches were compared considering their respective geometric limitations, time scales to manufacture, time scales to assemble, ease of assembly, and build dimensions - all crucial considerations to meet stakeholders' needs. Geometric limitation refers to the degree to which electronic components constrain the design of mechanical systems, and is important since enabling design freedom is crucial to meeting stakeholders' needs. The time scales for both manufacturing and assembly are also important for stakeholders to minimize. Stakeholders further desire 3 build dimensions and an easy assembly process. Electromechanical 3D printing is demonstrably the most optimal solution space from those considered since it meets or exceeds every stakeholder threshold, and therefore was selected for further exploration and subsystem downselection.

Conductive Material Selection

Most crucially, an optimal material family had to be chosen for printing the conductive traces. Materials considered were pure solder wire, liquid flux combined with solder, solder paste, copper paste, a silver colloid, and a custom material. As seen in *Table 5*, the quantitative characteristics these materials were compared on were expected system fixed cost, material variable cost, electrical resistivity, build dimensions, print speed, and required post-processing. Thresholds for these characteristics are derived from the stakeholder driven solution characteristics described in Section 2.2.

Table 5: Conductive Material Selection [1, 10, 16, 17, 28, 29, 30, 31]

Solution	Fixed Cost	Material Var. Cost	Electrical Resistivity	Build Dimensions	Print Speed	Req. Post Processing
Threshold	**$750**	**$65/kg**	**$50x10^{-8}$ Ωm**	**3**	**50 in/min**	**15 min**
Solder Wire	$700	$30/kg	$14.5x10^{-8}$Ωm	3	50 in/min	15 min
Liquid Flux	$750	$40/kg	$14.5x10^{-8}$Ωm	3	35 in/min	20 min
Solder Paste	$900	$35/kg	$25x10^{-8}$Ωm	3	40 in/min	15 min
Copper Paste	$900	$55/kg	$100x10^{-8}$Ωm	3	40 in/min	15 min
Silver Colloid	$1200+	$1000/kg	$50x10^{-8}$Ωm	2/3	120 in/min	10 min
Custom	$1500+	$100+/kg	$50x10^{-8}$Ωm	3	40 in/min	15 min

Better Than Threshold	At Threshold	Deviates Moderately	Non-Starter

Considering these metrics, solder wire is the most optimal material choice. From here, further research was conducted to select solder alloys to test with that have the best properties for the system. These research and testing efforts are elucidated in Section 5.2 below.

Insulative Material Selection

The other essential consumable material for this system is the insulative material used in creating the structural components of the 3D printed object. Narrowing down insulative material choices involved searching for plastics that are already available in filament form for 3D printers. These options are represented on the Ashby chart below in *Figure 4*.

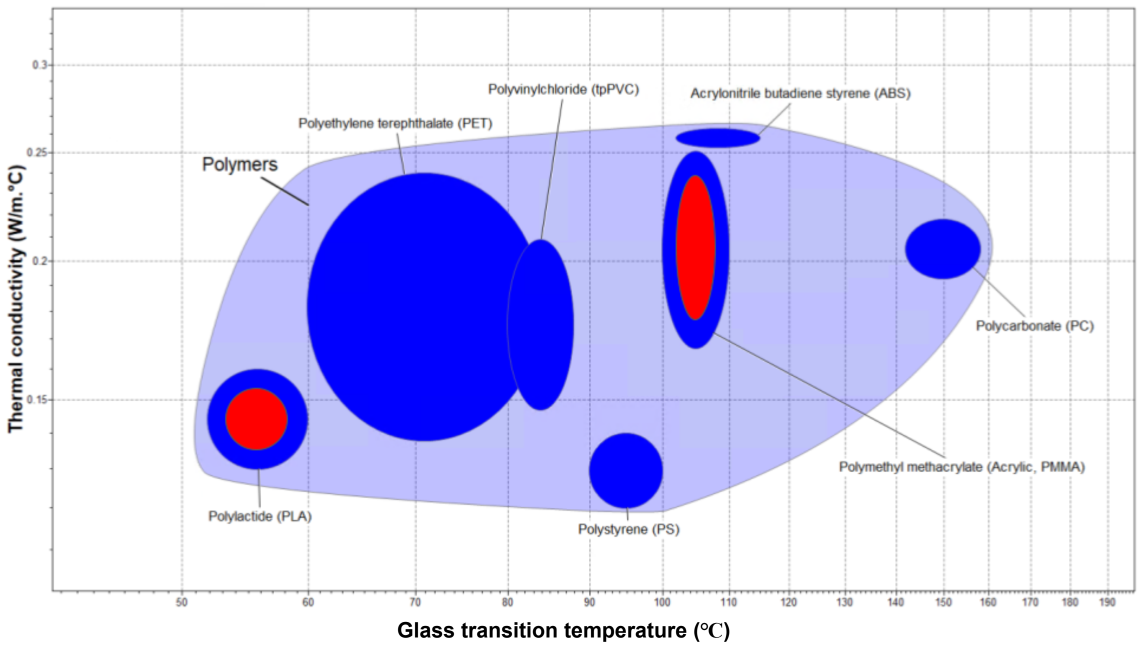

Figure 4: Insulative Material Selection

Testing a variety of thermal conductivity values and glass transition temperatures was essential for being able to experimentally determine how the conductive material of choice, solder wire, would interact with the insulative material. Polylactic acid (PLA) and polymethyl methacrylate (PMMA) were chosen because, between the two of them, they possess a wide distribution of thermal conductivities and glass transition temperatures. Most prints would be completed using PLA since it is one of the most common plastics for consumer 3D printers and is therefore the most readily available. Furthermore, the calculations in Section 3.3 shows that PLA is able to handle solder deposition without significant deformation or damage when using a selected cooling fan.

Hotend Selection

The basic operation of a 3D printer requires three mechanical components: the hotend, the extruder, and the nozzle. The hotend is the component of a 3D printer that melts the raw material in preparation for extrusion through the nozzle. Given cost and facility access constraints, as well as the fact that solder wire is not typically extruded using a 3D printer, it was necessary to find a hotend that fit a unique combination of filament size, cost, nozzle style, and temperature rating requirements. This downselection process is visualized in *Figure 5*.

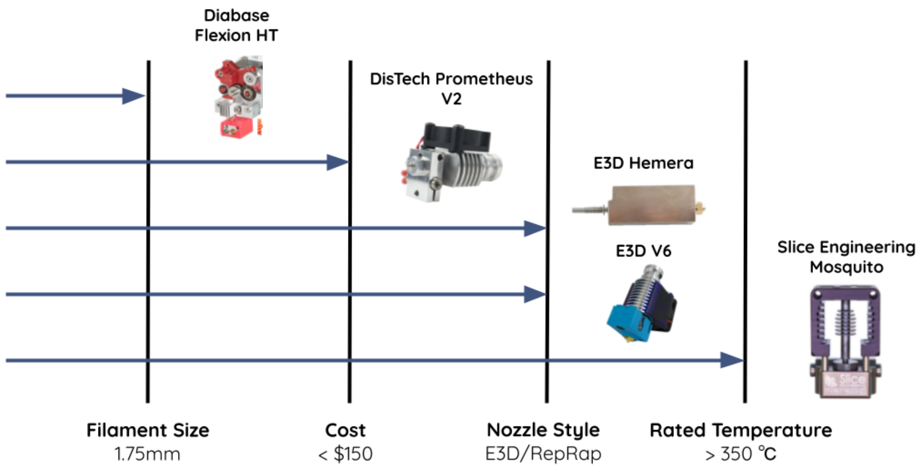

Figure 5: Hotend Selection [32, 33, 34, 35, 36]

The hotend needed to be designed for 1.75 mm filament since standard consumer 3D printers are designed either for 1.75mm or 3mm filament, and the largest diameter available in the solder alloys the team wanted to test was 0.063 inches, or around 1.6mm. A cost of less than $150 was needed to stay within the overall system fixed cost of $750 or less. The hotend needed to be compatible with the E3D (also called RepRap) 3D printer nozzle style since the optimal nozzle choice was only available in that style. A rated temperature of over 350°C was required to ensure the system could comfortably melt all solder alloys during testing. The team proceeded with the Slice Engineering Mosquito hotend as it met all of these requirements.

Extruder Selection

The extruder is the component of a 3D printer that feeds the filament into the hotend for melting. The team searched for an extruder that met requirements relating to motor compatibility, footprint, complexity, and fixed cost, as seen in *Figure 6.*

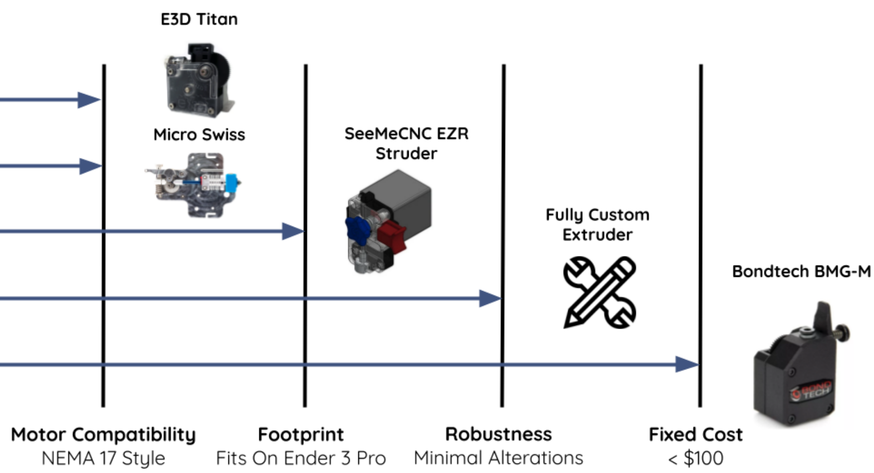

Figure 6: Extruder Selection [37, 38, 39, 40]

The extruder needed to be compatible with a NEMA 17 style motor since these motors are a typical choice for use in consumer 3D printers and hence are cheap and readily available off-the-shelf. The dimensions of the extruder needed to permit mounting on an Ender 3 Pro, as this is the 3D printer that the team retrofitted, as described further in Section 4.1. Maximum robustness was sought by minimizing the number of alterations or additional adaptors that would be required to retrofit the printer. Finally, a fixed cost of under $100 was needed to stay within the overall system fixed cost requirement. The team selected an extruder that met all of these requirements: the Bondtech BMG-M.

Nozzle Selection

The nozzle is the component of a 3D printer that deposits the molten raw material onto the build plate or workpiece. Given that this system extrudes solder wire instead of plastic, it had unique requirements for the nozzle relating to abrasion resistance, rated temperature, wettability, and corrosion resistance. This downselection process is shown below in *Figure 7*.

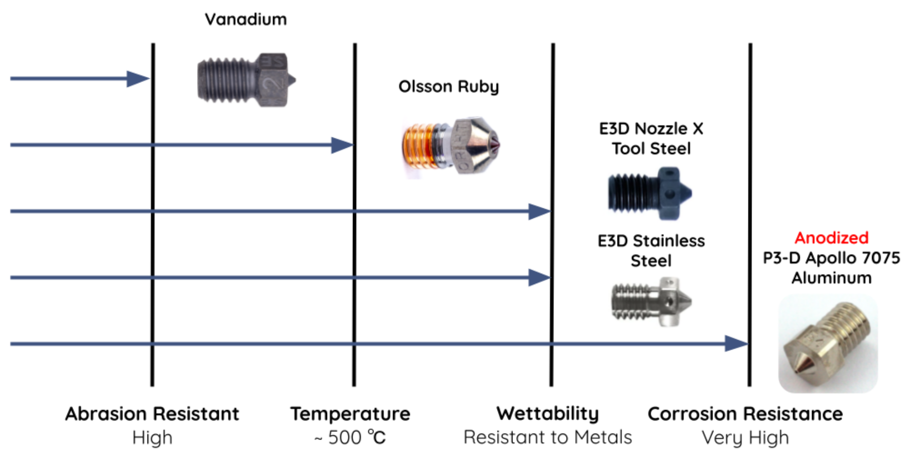

Figure 7: Nozzle Selection [41, 42, 43, 44]

The nozzle needed to be highly resistant to abrasion and corrosion in order to ensure that the aperture would not be compromised by the molten solder. A rated temperature of around 500℃ was also required in order to accommodate all solder alloys during testing. Finally, the nozzle needed to be made from a material resistant to wetting with metals to ensure that the solder would flow through the nozzle and not adhere to it. One benefit of anodizing is that it improves resistance to wetting with metals by forming an oxide layer on the aluminum. Hence, when anodized, the P3-D Apollo 7075 aluminum nozzle would meet all these requirements; however, since anodized nozzles are not available on the market, the P3-D nozzles were anodized with the help of a team sponsor, Hillock Anodizing.

3.2. Quantitative Analysis - Solder Deposition

Solder Deposition and Flow Regime

Solder deposition is not as simple as typical FDM 3D printing. Indeed, solder deposition, as will be experimentally shown in Section 3.4, occurs dropwise; this process is represented in diagram form in **Appendix A4**. One of the key quantitative parameters that underlies solder extrusion is the Weber number, which represents the ratio of fluid inertia to surface tension. It is defined in equation (1) as:

$$\mathrm{We} = \frac{\triangle \rho v^2 d}{\gamma} \propto \frac{\text{fluid inertia}}{\text{surface tension}} \tag{1}$$

where γ is the interfacial surface tension in N/m, v is the velocity in m/s, d is the nozzle diameter in m, and $\Delta\rho$ is the difference in density between metal and surrounding fluid in kg/m^3 [45]. As shown in *Figure 8*, the Weber number determines if solder is extruded as a drop, as connected drops, or as a wire.

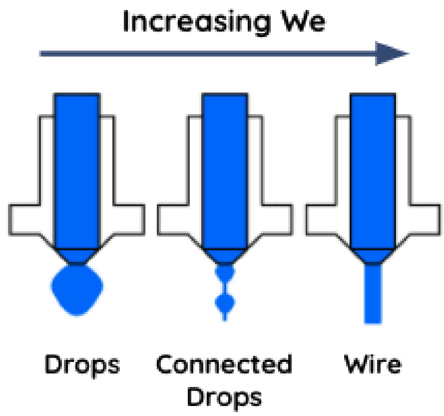

Figure 8: Solder Flow Regimes

The wire regime corresponds to a Weber number of 6 x 10^{-1} [45]. Using the properties for the Sn-60Pb-40 solder alloy, where γ is 468 dynes/cm at 330 ℃ (which is equivalent to 468 mN/m), ρ_{solder} is 6800 kg/m^3, and ρ_{air} is 1.225 kg/m^3 (corresponding to a $\Delta\rho$ of 6798.78 kg/m^3), along with the Bondtech BMG-M's 3:1 gear ratio and 4.7 mm gear radius, the feed motor would need to operate at 474 rpm to achieve solder flow in the wire regime [46]. This corresponds to 548 inches of solder wire being extruded per minute, or around 9.1 inches per second, which is not feasible for the current system: heat cannot be transferred to the solder fast enough to melt it at that feed rate.

A more reasonable speed for this extruder motor is on the order of 20 rpm. This results in a Weber number of 1.187 x 10^{-4} using the same properties discussed above, which corresponds to operation in the drop regime. While operating in the wire regime could result in greater efficiency and precision in depositing conductive traces, it was determined that all project goals could effectively be achieved in the drop regime without the added complexity of reaching the wire regime. The key parameter for analyzing solder deposition in the drop regime is the Bond number, which represents the ratio of gravity to surface tension. The Bond number is defined in equation (2) as:

$$\mathrm{Bo} = \frac{\triangle \rho g L^2}{\gamma} \propto \frac{\text{gravity}}{\text{surface tension}} \tag{2}$$

where γ is the interfacial surface tension in N/m, L is the characteristic length (drop radius) in m, g is gravitational acceleration in m/s^2, and $\Delta\rho$ is the difference in density between the metal and surrounding fluid in kg/m^3 [47]. The Bond number determines when a drop in the drop regime falls from the nozzle; this occurs when the Bond number is around 1. For the same solder properties described above, this corresponds to a drop diameter of 4.71mm, which represents the resulting trace width. Ideally, this diameter would be as small as possible to allow for printing of smaller trace widths, but it is primarily dictated by the material properties of the solder as well as the optimal nozzle geometry. Changing both of these parameters is quite complex, and hence will be left as a next step for this project.

Hotend Temperature and Feed Rate

Building on the above solder deposition model, critical calculations were performed to determine what temperature settings to use for the selected hotend and what solder feed rates could be used at each given temperature. As discussed in Section 3.1, the selected hotend was picked for its capability to extrude at temperatures greater than 350°C and even up to 500°C since the team was particularly interested in performing a parameter sweep of many different extrusion temperatures. For that reason, this analysis considered all temperatures in this range.

The following thermodynamic analysis used a lumped capacitance model to represent the heat transfer between the hotend and the solder alloys as well as the heat transfer within the solder "lumps." The analyzed length of solder extruded through the hotend was selected to satisfy the main assumption of the lumped capacitance model: that the Biot number, the ratio between the resistance to heat flow within the solder lump and the resistance to heat flow into the solder lump, should be less than or equal to 0.1. To that end, a Biot number of 0.05 was selected and used to calculate the length of solder that could be extruded under these assumptions. Since heat flow within the solder lump is critically defined by its cross-sectional area, the area of heat transfer was considered as a circular cross-section, or πr^2, with r representing the radius of the solder, equal to 0.8 mm for all selected alloys. Furthermore, since heat flow from the hotend to the solder lump can only occur across the cylindrical walls of the solder, the area of heat transfer was considered equal to the lateral surface area of the cylinder, or $2\pi rh$, with r defined above and h equal to the height of extruded solder in each individual lump. With the above defined Biot number and the equations for heat transfer across both mediums, this solder height was calculated to be between 0.003" and 0.004" for each solder alloy used.

With this extrusion length defined, the lumped capacitance model was then used to analyze heat transfer within the solder independently of the heat transfer from the hotend. The simple conductive heat transfer equations from [47] were used to analyze heat transfer within the solder alloy, as shown in equation (3) below, where k represents the conductive heat transfer coefficient between the interfaces, A represents the area of heat transfer, L is the length over which this heat transfer occurs, and T_1 and T_2 represent temperature at different time steps.

$$q = -kA\frac{T_2 - T_1}{L} \tag{3}$$

From here, this heat transfer equation was manipulated into the form of equation (4) below, which is particularly useful for calculating steady state temperature change since heat transfer is proportional to heat capacity multiplied by temperature.

$$\frac{\mathrm{d}Q}{\mathrm{dt}} = C\frac{\mathrm{d}T}{\mathrm{dt}} = mc\frac{\mathrm{d}T}{\mathrm{dt}} = -kA_{CS}\frac{T_\infty - T(\mathrm{t})}{L} \tag{4}$$

Analytically solving this equation found the rate of change of temperature over time, which precisely determined how fast this system could deposit solder, and led to equation (5) below. In this equation, T_∞ corresponds to the heat source temperature, or the hotend temperature in this case; T_0 corresponds to the initial temperature of the solder, or 25°C in this case; and t corresponds to the time after the solder lump begins contacting the hotend.

$$T(\mathrm{t}) = T_\infty - (T_\infty - T_0)\mathrm{e}^{-793.42\mathrm{t}} \tag{5}$$

This analytical solution can be used to solve for the approximate temperature of a solder "lump" after t seconds of heat transfer from the hotend, where each lump has a height of between 0.003 and 0.004 inches as calculated above. It may be noted that the resulting time constant for this system is particularly large; however, this result is physically sound when considering that the solder lump has an extremely small height. Deriving equations of similar form for a significant number of solder alloys produced *Figure 9*, which represents the maximum feed rate for each solder alloy at each temperature.

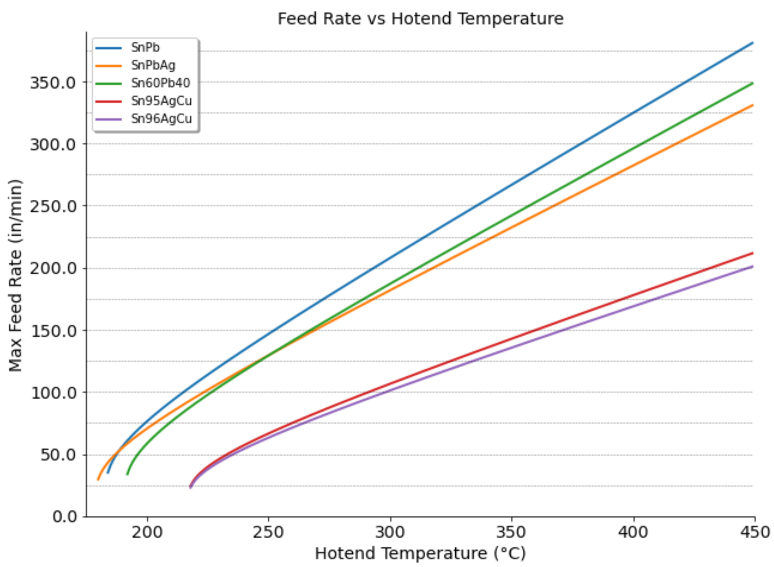

Figure 9: Max Solder Feed Rate at each Temperature, for Labeled Solder Alloys

This feed rate was derived using the above temperature equation, with T(t) selected to be only 1°C larger than the melting temperature of each solder, since each alloy only had to reach its melting temperature to be extruded. Once all other variables in the equation were determined, the time t could be calculated to reach this desired temperature. As described above, this time is the minimum amount of time required to heat a solder mass of height h to its melting temperature; then, time and solder height can be used to determine the maximum feed rate.

3.3. Quantitative Analysis - Conductive/Insulative Material Heat Transfer

Cooling of Solder Traces

An important consideration for this project was ensuring that any deposited solder traces would cool sufficiently quickly, both so that solder deposition could continue and so that any heat transfer to the insulative material would be minimal and not cause deformation. Equation (6) below is the Nusselt equation for forced convection over a cylinder, a non-dimensional equation that can be used to model convection cooling via a cooling fan, which was proposed for cooling the deposited solder.

$$\mathrm{Nu}_{\mathrm{cyl}} = \frac{hD}{k} = 0.3 + \frac{0.62\mathrm{Re}^{1/2}\mathrm{Pr}^{1/3}}{[1+(0.4\mathrm{Pr})^{2/3}]^{1/4}}[1+(\frac{\mathrm{Re}}{282,000})^{5/8}]^{4/5} \tag{6}$$

In this equation, h represents the heat transfer coefficient for the forced convection; D represents the diameter of the characteristic cylinder; k represents the conductive heat transfer coefficient of the solder alloy; Pr represents the Prandtl number, a constant for the regime of air in this system; and Re represents the Reynolds number, a variable which changes significantly depending on the characteristics of the cooling fan selected.

The team studied a variety of cooling fans to select one with an appropriate operating Reynolds number for generating a large enough heat transfer coefficient, thereby maximizing the heat lost to convection. To do so, the cooling fan would need a Reynolds number greater than or equal to 12.3, derived from determining the minimum heat transfer coefficient to ensure the solder and PLA are cooled fast enough from equations (13-16) and (17-20). This Reynolds number corresponds to a volumetric flow rate of roughly 38 cubic feet per minute (CFM), calculated by considering the diameter, pitch rate, and RPM of typical 3D printer fans. For this reason, the team selected an 80 mm cooling fan with a volumetric flow rate of 69.2 CFM to provide a large safety factor. Using equation (6) to calculate the heat transfer coefficient with this fan leads to a value of h = 68.5 W/K-in^2.

Using this coefficient, the convective heat transfer per unit length of solder can be calculated from the heat transfer equations [47]. The critical variables of this equation are the surface area per unit length A' = πr, derived as half of the lateral surface area of a cylinder per unit height, and radius r of 0.01 inches, derived from a minimum trace width of 0.02 inches from standard PCB manufacturers [48, 49, 50]. The convective heat transfer from cooling is then calculated below in (7-9):

$$q' = hA'(T_{\mathrm{surf}} - T_{\mathrm{a}}) \tag{7}$$

$$q' = 68.5\mathrm{W/K\text{-}in}^2 \text{ x } (\pi \text{ x } 0.01\mathrm{in}) \text{ x } (350°\mathrm{C} - 25°\mathrm{C}) \tag{8}$$

$$q' = 699\mathrm{W/in} \tag{9}$$

The results of the above calculations show that 699 W of heat are lost per inch of solder deposited due to the inclusion of the cooling fan used in this system. To prove that this heat transfer is sufficient to minimize deformation of the plastic, it is compared to the conductive heat transfer to the insulative material, assumed to be PLA. This is modeled per unit length of solder deposited in equations (10-12):

$$
\begin{aligned}
q' &= -kA'\frac{T_{\text{PLA}} - T_{\text{solder}}}{\triangle x} &\text{(10)}\\
q' &= -0.13\text{W/m-K x } (\pi \text{ x } 0.01\text{in}) \text{ x } \frac{(25°\text{C} - 350°\text{C})}{0.015\text{in}} &\text{(11)}\\
q' &= 88.5\text{W/in} &\text{(12)}
\end{aligned}
$$

where k_{PLA} = 0.13 W/m K, the unit surface area is the same as for convective heat transfer equations (7-9), and Δx = 0.015 inches is the minimum layer thickness of PLA upon which a trace would be deposited. Hence, the ratio between convection and conduction is 7.9, which shows that convection is by far the dominant mode of cooling. The required time it would take to cool the solder trace is calculated with the steady state heat transfer equation [51] in equations (13-16):

$$
\begin{aligned}
\rho c_p \frac{\partial T}{\partial \text{t}} &= \sum q'/A &\text{(13)}\\
28.38\,\text{J/K-in}^3 \text{ x } \frac{\partial T}{\partial \text{t}} &= \frac{699\text{W/in}}{(\pi \text{ x } 0.01\text{in})(0.015\text{in})} + \frac{88.5\text{W/in}}{(\pi \text{ x } 0.01\text{in})(0.015\text{in})} &\text{(14)}\\
\triangle T &= 58900\text{K/s} \triangle \text{t} &\text{(15)}\\
\text{t}_{\text{cool}} &= \frac{(350°\text{C} - 25°\text{C})}{58900\text{K/s}} = 0.005\text{s} &\text{(16)}
\end{aligned}
$$

The additional variables in these equations are the density of the eutectic SnPb solder, $\rho = 7.4$ g/cm^3, its heat capacity, c_p = 0.234 J/g-K [51], and the temperature gradient over cooling solder deposited at 350°C. The results of this calculation demonstrate that the solder should cool to roughly room temperature within 1/200-ths of a second. The following calculations will show heat transfer into the PLA during this time window.

PLA Heat Transfer

Previously, it was determined that conductive heat transfer per unit length to the insulative plastic was 88.5 W/in and that the solder traces cool within roughly 1/200-th of a second with a cooling fan. This was validated experimentally by depositing a solder bead onto a PLA coupon, and finding that it cooled extremely quickly and did not cause any damage or warping to the coupon. Using equation (9) with PLA material properties of density $\rho = 1.24$ g/cm^3 and heat capacity c_p = 1.8 J/g-K [52], the change in temperature of the PLA is shown in equations (17-20) below.

$$
\begin{aligned}
36.58\,\text{J/K-in}^3 \text{ x } \frac{\partial T}{\partial \text{t}} &= \frac{88.5\text{W/in}}{(\pi \text{ x } 0.01\text{in})(0.015\text{in})} &\text{(17)}\\
\frac{\partial T}{\partial \text{t}} &= 5130\text{K/s} &\text{(18)}\\
\triangle T &= 5130\text{K/s x } 0.005\text{s} &\text{(19)}\\
\triangle T_{\text{PLA}} &= 28.3\text{K} &\text{(20)}
\end{aligned}
$$

Beginning with cooled PLA at 25°C, a change of 28.3°C corresponds to a final temperature of 53.3°C - close to, but nonetheless under, the glass transition temperature of PLA, 57°C. In order to prevent heated material from reaching the glass transition temperature, one of several measures could be taken: another insulative material with a higher glass transition temperature could be used instead, or the cooling system could be made more effective to cause more heat loss to convection and minimize the heat transfer due to conduction. However, during validation testing, warping did not occur past a very small, localized area, and this warping may have indeed helped with solder adhesion, therefore indicating that the team did not need to implement either of these changes.

3.4. 1D Gantry Validation Testing

A one dimensional test gantry was designed and manufactured to test the feasibility of the selected combination of hotend, extruder, and nozzle that comprise the solder deposition system. This test gantry operated by simply moving in a straight line along a pair of high tolerance ground rods. Using this test gantry allowed for experimental validation of the above quantitative analyses for the solder deposition model and heat transfer involved in this project. Images of both the rendered and final built test gantry can be seen in *Figure 10*.

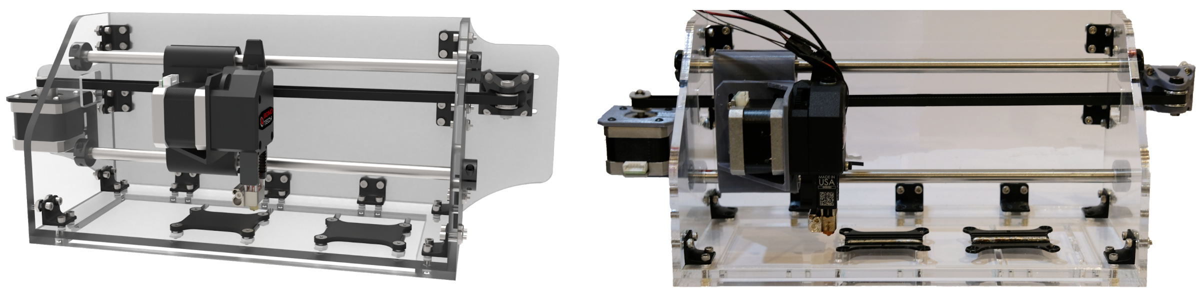

Figure 10: 1D Test Gantry - Rendered (left) and Built (right)

This 1D test gantry was further used to experimentally determine several essential properties for successful project execution: speeds and feeds of extrusion, extrusion temperature, channel deposition geometry, nozzle to build plate height, nozzle aperture, trace resistance and continuity, and material wetting characteristics. The extruder system is controlled from an Arduino with custom designed circuitry and software controls. This circuit powered two NEMA 17 stepper motors, one for feed and one for speed, two joysticks for manually controlling the steppers when desired, the hotend heater cartridge, and the hotend thermistor. The circuit schematic and actual electronic controls can be seen in **Appendix A5**.

The data collection process for determining these essential parameters involved first finding the optimal extrusion temperature for each solder alloy, and then systematically varying nozzle aperture between different sized anodized aluminum nozzles, varying nozzle height by adjusting slot screw location, varying the speed of movement and the feed of deposition, and varying the channel radius. The optimal channel radius in particular was essential to determine since the channel geometry would help entrap the solder wire and prevent it from spreading out as it wets via localized melting to the plastic. Test coupons were developed using a standardized print profile and were then 3D printed out of both

PLA and PMMA with varying channel geometries. In total, 10 different test coupons were tested with, the best 6 of which can be seen in *Figure 11.*

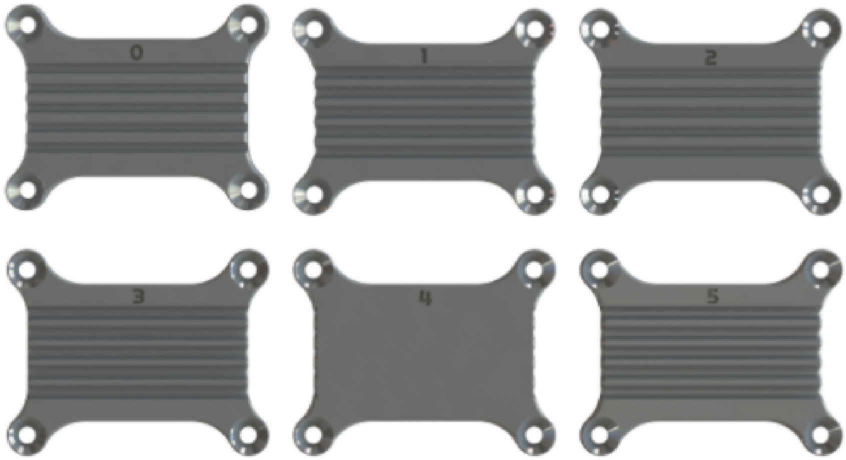

Figure 11: Test Coupon Geometries Used on the 1D Test Gantry

Once solder extrusion was conducted, resistance and continuity measurements were made for each trace and wetting adhesion was tested with a shallow drop test. Detailed quantitative and qualitative testing data for these 6 test coupons can be found in **Appendix A6**. The biggest takeaways from 1D test gantry experimentation can be summarized as follows:

1) Solder extrusion occurred dropwise, and trace diameter aligned with theory and calculations. Extruding at the wire regime would not be possible using reasonable feeds and speeds and hence extrusion was not as simple as FDM printing, requiring more careful testing.

2) The anodized aluminum nozzle was selected as the optimal printing nozzle after testing non-anodized and anodized aluminum, brass, and steel nozzles. The optimal solder extrusion aperture was 0.6mm to avoid excessively large trace sizes, poor deposition, and nozzle clogging.

3) A wide channel geometry with a 0.075" radius and a nozzle to build plate ΔZ height of 0.125" were found to give the best consistent printing results with the above parameters defined.

4) Solder adheres to the plastic wafer due to localized melting at the surface of the coupon, and this wetting was better with PLA than PMMA, so PLA was selected for further testing at this stage. Despite the calculations in Section 3.3, the team forewent the use of forced convection cooling at this time for the sake of quick prototyping with the test gantry; as a result, some warping was observed on the PLA, so this cooling was implemented into our full build.

4. Final System Form

4.1. 3D Implementation Gantry

After successfully testing on the 1D platform and modeling solder extrusion, a 3D gantry was developed to implement full three dimensional capabilities. This was accomplished by retrofitting an Ender 3 Pro with the extruder system developed for the 1D test gantry, incorporating an active cooling fan to allow for forced convection cooling, and adding an independent second extruder head for extruding plastic alongside the solder wire. The team strategically partnered with a company called SEN3D to develop and install this second extrusion system for the printer. The Ender 3 Pro was identified as the 3D printer platform of choice for three reasons: it is fully open-source, several team members already had intimate knowledge of this specific printer, and there exists a large online community for making modifications to this specific printer. Pictures of this build can be seen in *Figure 12* below.

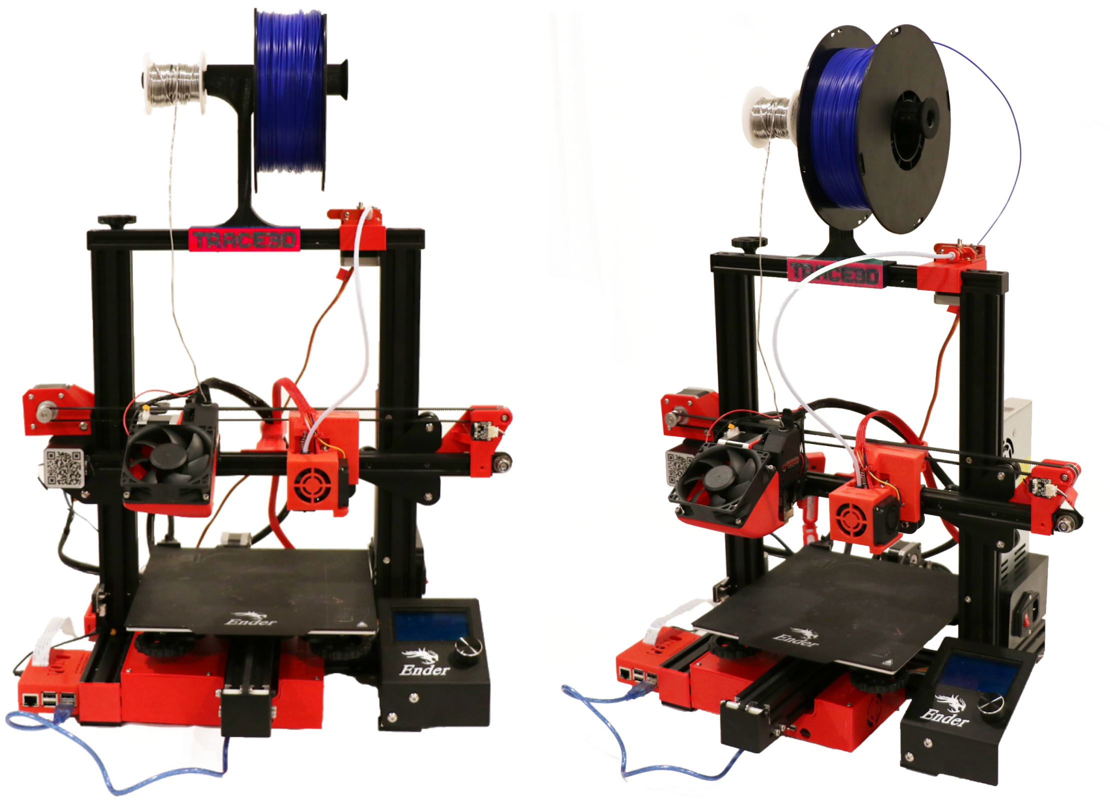

Figure 12: 3D Implementation Gantry

This printer was controlled using G-Code commands, which are simple snippets of code that interface with the printer's open-source firmware, Marlin. This process is described in much more depth in Section 4.2 below. To initially test on this platform, a series of parameter tuning experiments were performed in both 1D and 2D using specially developed acrylic test beds. These beds were datumed on the Ender 3 Pro's bed via four 0.5" locating pins that were printed and adhered directly onto the build plate. Then the acrylic test beds were placed and automatically centered such that all test coupons could be located in space and extruded onto, which can be seen in *Figure 13* below.

Figure 13: Acrylic Test Bed

This parameter tuning process for calibrating the printer is described in further detail in Section 4.3.

4.2. G-Code Generation

To work with the 3D gantry described in Section 4.1, the team created G-Code generation tools that interfaced directly with the printer's firmware.

Octoprint

An open-source web interface, Octoprint, was first installed and configured to allow commands to be sent over WiFi from a laptop to the printer, enabling quick and easy testing of different commands, settings, and functions. Using Octoprint, some of the most relevant commands for our purposes were determined and are defined below [53]:

1. **G01** - command to move linearly in three dimensions while extruding
2. **G02/G03** - command to move in a clockwise/counterclockwise arc while extruding
3. **G04** - the "dwell" command, which sets the extruder to delay without moving or extruding
4. **G92** - command resets the cumulative amount of material extruded in the printer's firmware
5. **M106** - command to turn on the cooling fan and configure its speed
6. **M206** - command used to set the firmware's "zero position" for the extruder position

Using these commands allowed the team to determine and implement the appropriate settings for printing with solder. While becoming familiar with these individual commands was essential for understanding the basic components of the printing process, it was still necessary to combine these commands in an intelligent series to complete an entire print. To this end, several programs with different capabilities for generating G-Code commands were developed.

MATLAB

The first of these programs was a MATLAB script that was capable of producing a series of commands to print onto circular channels, which will be detailed more in Section 4.3. MATLAB was initially selected due to the heavy computational nature of generating these commands in such a way as to break up the desired circle coupon into much smaller arc segments to analyze the solder deposition over the entire geometry. Generating the circle G-Code was accomplished using the G02 and G03 commands over short distances, effectively chopping the circle into 10 to 30 small angle increments. Between each of these circular move-extrude commands, dwell commands (G04) were spliced into the script to allow the extruder to briefly pause after extruding one segment to allow the subsequent solder droplet to form and solidify.

While sending commands with Octoprint provided some familiarity with G-Code and how to use it, testing with this MATLAB script allowed the team to determine which settings to use for each command to create a successful print, such as the necessary amount of material to extrude over each circle segment and how long each segment should be. Using this script also proved that it was possible to computationally map the setting from an arc, using G02 and G03 commands, onto a straight line, using G01 commands, while retaining the same successful print results. This further allowed the team to tune parameters for printing in three dimensions, which is once again detailed in Section 4.3 below.

Solder Bridging

After developing a base for computing and generating G-Code commands for printing solder successfully, the team moved onto creating a more reliable set of programs with more advanced functionalities. Henceforth, all programming for Trace3D was completed in Java in order to develop a more reliable user interface with modular, reusable code. The first program developed in Java was a "bridger;" a program capable of printing the insulative plastic material as a "bridge" over deposited solder. The results of prints with this method can be visualized in *Figure 14*, a preview of the test print totem described in Section 5.2 below.

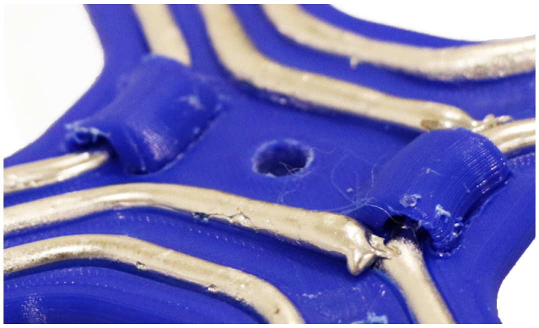

Figure 14: Bridging Test Results on Final Totem

Since solder is deposited in predefined channels in the plastic base, and since it would need to be encapsulated in the final form to ensure that electronics are not exposed and to allow for true 3D printing, this program is essential for the safety and long-term viability of the team's vision for the final system. Demonstrating that this concept is feasible was merely the first step. This Java-based bridging tool is capable of modifying the G-code files generated by another slicer, such as Cura, and is not yet able to generate its own complex 3D slices from the ground up. Since slicers such as Cura are only designed for 3D printing with plastic material, and are not automatically configured to incorporate the second extrusion system or the deposited solder wire, the bridging tool modifies the PLA extrusion files to cause all movements which would otherwise collide or interfere with the deposited solder to be moved out-of-plane and "jump" across the wire as necessary.

Java Slicer

To ultimately solve the limitations of the aforementioned slicers, the final program developed for Trace3D G-Code generation was a Java slicer capable of producing an entire arbitrary G-Code profile based on a set of manually inputted coordinates in space. There were several significant advantages to developing this slicer as opposed to configuring settings in an existing slicer like Cura. One of the most significant is that this method allows for complete translation of parameter tuning results into a working print, while configuring Cura would still require post-processing steps such as what was done to accomplish bridging. Additionally, developing a custom slicer allows the team to scale quicker: working with simple MATLAB scripts would be difficult for users to interface with and would eventually require significant modifications for different profiles. Creating a custom slicer in Java is the beginning of what could eventually become the slicer for the proposed final system form. Java also afforded the team better tools for creating a graphical user interface (GUI) by using Java Swing, which is far more user-friendly than MATLAB's GUI capabilities. *Figure 15* shows the process of using this slicer to create solder traces in a 2D plane, but this slicer also has the capability to generate 3D profiles like other slicers might. In these diagrams, black lines represent the solder path and red lines represent tool path jumps between different traces.

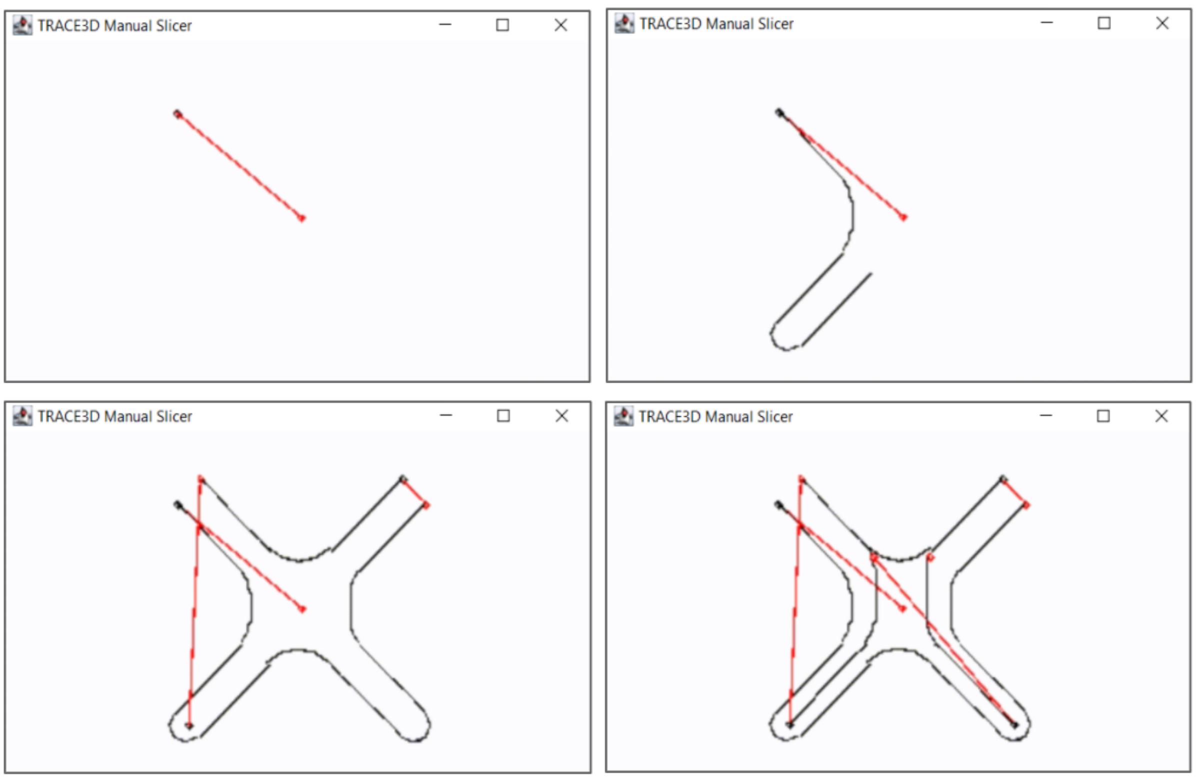

Figure 15: Manual Slicer Building up Solder Trace Profiles

4.3. Parameter Tuning

Parameter tuning of all pertinent 3D printer settings via G-Code generation was essential for moving from experimenting with simple command strings to creating successful prints in 2D and 3D. Most tuning was accomplished using the MATLAB script described in Section 4.2 for creating circular test prints. These circular profiles were printed onto PLA test coupons that were either printed with the 3D gantry directly or printed independently and affixed to the build plate via locating pins (see Section 4.1, *Figure 13*). These circle coupons can be seen in *Figure 16*, which shows how the tuning progressed over multiple iterations of solder alloys, coupon geometries, and extrusion parameters.

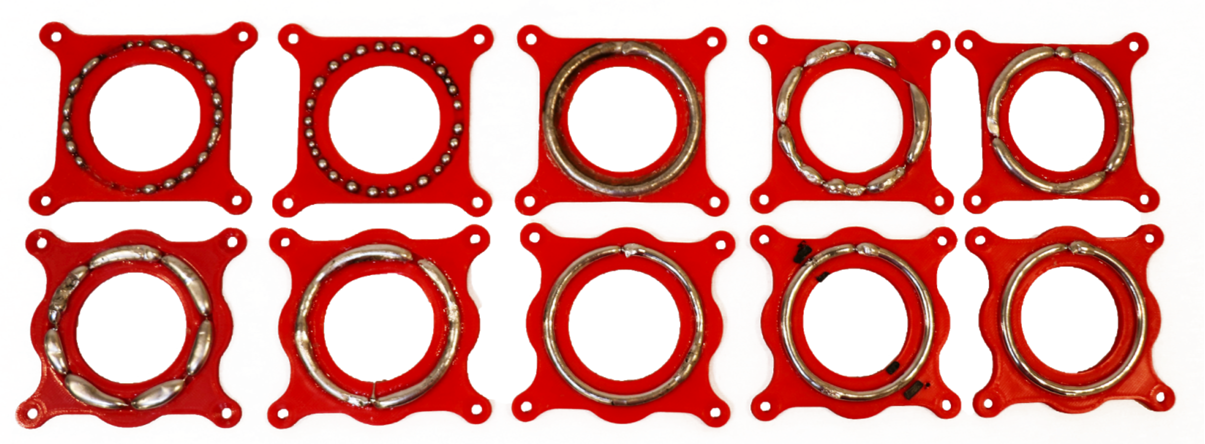

Figure 16: Circular Coupon Iterations, with Variable Geometries and Solder Alloys

The three top-left-most coupons show iterations of the same coupon geometry and solder alloy. The first parameter that was altered was the extrusion rate, controlled by a setting on each of the movement commands (G01, G02, G03) detailed in Section 4.2 that corresponds to the cumulative amount of solder extruded over all movements. For each subsequent test, more material was deposited into the channels by increasing the amount of extruded solder between movements. Since the extrusion amount is stored as a cumulative sum in the printer's firmware, the G92 command became useful to reset the state of the extruder between tests, effectively zeroing out this cumulative amount.

The two top-right-most coupons contain a slightly different solder alloy, which are visibly lighter and have a better surface finish than the top-left coupons. This change is due to a few reasons, the most significant of which is that the solder in these coupons does not contain flux and instead comes from a solid-core wire. The reasons for switching to this solder are detailed in Section 5.1, but the switch was made primarily due to the better surface properties intrinsic to this alloy. Notably, after switching solder alloys, printed trace continuity was slightly worse, which required more tuning of extrusion amounts, as described above, to amend.

Finally, the bottom five coupons show more iterations for a more optimal coupon geometry. The new channel geometry reduced solder overflow outside of the channel by adding a flanged top to ensure the printed solder was properly embedded into the channel. This change allowed for more compliance for the gantry movements and further constrained the solder to the channel. With these test coupons, iterations included changes in the speed at which the printer axes moved during the print, corresponding to a setting on each of the movement commands (G01, G02, G03), and changes in the delays between each movement command, corresponding to a setting on the dwell commands (G04). These iterations led to better printed trace continuity, better surface finish, more adhesion within the printed channels, and more consistent results across prints.

After completing parameter tuning to achieve consistent results on the circular coupons for the selected solder alloys, similar parameter studies were performed on several other solder alloys. The results of this testing are presented in Section 5.1. Additionally, after completing this parameter tuning over two dimensions, the results were easily translated to one dimensional prints along the X, Y, and Z axes with the Trace3D manual slicer, which is described in Section 4.2.

4.4. Future Iterations

For future iterations of Trace3D, we designed a tentative final system form customized gantry with two independent extruder heads and a dual-Z drive, as visualized in *Figure 17.*

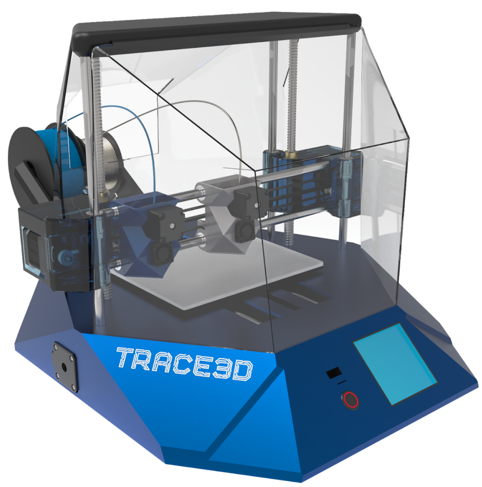

Figure 17: Final System Form in CAD

The whole assembly is partially enclosed to provide protection from the hot solder being deposited and reduce exposure to any fumes that may be produced. This concept uses a plastic unibody lower construction to save on manufacturing costs while providing a striking visual appearance, and uses an LED touchscreen to simplify the user experience. Additionally, the gantry is designed to allow each extruder assembly to clear the build area completely to allow both extruders total access to the build volume. To ensure the smoothest possible operation during printing, the printer uses precision ground guide rods on all axes of movement with linear ball bearings to limit irregular loading on the stepper motors as well as constrain the extruders' and bed's motion along the intended axis to the greatest extent possible. At the rear there is a mount for the spools of the conductive solder as well as the plastic insulative material, which are easily replaceable when the materials run low or are exhausted.

5. System Performance

5.1. Material Exploration

The team contemplated a wide range of solder alloys to explore during material testing sessions, including five commonly used alloys and five unique alloys with low melting points. The five common alloys are represented in *Figure 9* of Section 3.2, which shows results for the heat transfer calculations for each alloy. Of these candidate materials, the solid-core eutectic Sn-63Pb-37 solder was found to be the best for multiple reasons. One of the most significant reasons was the lack of flux in this material, as some Rosin flux-cored solders caused hazardous fumes that were emitted when melted by the extruder system. Proper safety precautions and ventilation were used to test these alloys; however, it was still not sustainable. Additionally, the solid-core solder wire was more alluring with a much nicer surface finish, while the flux-cored wires had some tarnishing on the surface of the solder and the PLA. Indeed, the flux made it nearly impossible for more plastic to be adhered on top of the deposited base. As can be seen from *Figure 9*, the Sn-63Pb-37 solder has the best performance and highest slope on the plot, allowing for higher feed rates at each temperature with this alloy. Its melting temperature is the lowest of all the other tested alloys except when silver was added as an alloying element; still, since the eutectic alloy is the most commonly available and least expensive, this alloy was selected.

The team also experimented with some more unique solder alloys, which are not shown in the calculation results of Section 3.2 but with which similar calculations were performed. These alloys included Sn-42Bi-58, Sn-42Bi-57Ag-1, Sn-12Bi-49In-21Pb-18, Sn-48In-52, and Sn-40In-40Pb-20, all of which were acquired with the help of a team sponsor. Testing these alloys showed some unfortunate results: three of the alloys performed extremely poorly with Trace3D's extruder system and were complete non-starters. These were all alloys containing Indium content higher than 20%: each of these alloys was too soft to perform well with our extruder, and would jam in the extruder system before being deposited. The melting temperatures of these alloys were between 60 and 120℃, and could likely have produced good results with a custom extruder system. At this point the remaining two candidate alloys were Sn-42Bi-58 and Sn-42Bi-57Ag-1. The bismuth content in these alloys made them great contenders for this proposed system, as their melting temperatures were much lower than that of the tested SnPb solder. The testing results of each of these alloys are shown in *Figure 18* below, compared to the results of the eutectic SnPb solder selected.

Figure 18: Solder Alloy Selection; from left to right: Sn-42Bi-57Ag-1, Sn-42Bi-58, Sn-63Pb-37

Unfortunately, the team only had a small amount of each of these unique alloys to test with, so full parameter sweeps to optimize the results for each could not be performed. The results above use the optimized parameters for use with the selected SnPb solder. While some more optimization may benefit the performance of the other alloys, the surface finish of both Bismuth-containing alloys was much worse than that of the SnPb solder, likely due to some inherent properties of the solder. Given that these alloys are less available and the immediate testing results were not as good as expected, the eutectic SnPb solder was confidently selected as the best choice for Trace3D at this time.

5.2. Test Print Totem

Once an optimal material was selected, parameters were sufficiently tuned, and the custom slicer was completed, the retrofitted Ender 3 Pro was ready to be used for Trace3D printing. The "totem," or representative print to demonstrate the 2D and 3D printing capabilities in a complex part for this system, was a simple quadcopter. This drone is largely composed of plastic, with channels and vias built into its body for solder deposition. Renderings of this drone can be seen in *Figure 19.*

Figure 19: Drone Totem CAD, Isometric Top View (left) and Bottom View of Channels (right)

Once this drone was sliced, and the plastic body was manufactured on the 3D Implementation Gantry build plate, it took several iterations to actually get the printer to work. The team worked through the printer jamming, running into nubs on the part, issues with the slicer handling complex geometries, zeroing incorrectly, and creating discontinuous traces - these iterations can be seen in **Appendix A7.**

However, eventually the drone printed successfully. A timelapse of the print can be seen using this link here. First, the printer creates the plastic drone chassis, then it proceeds to deposit solder in the Z-axis vias. This is soon followed by the deposition of solder into the printed channels using the trace profile ran through the Trace3D custom slicer to create the conductive pathways. Plastic material is then bridged over the solder to fully cover it, as was described in Section 4.2. Continuity is checked to ensure that the drone can actually function, and post-processing for this totem simply involved connecting the motors and batteries to the deposited solder wire, thus creating a closed circuit and enabling the drone to turn on. Images of this final drone totem can be seen in *Figure 20* below, and more can be found in **Appendix A8.**

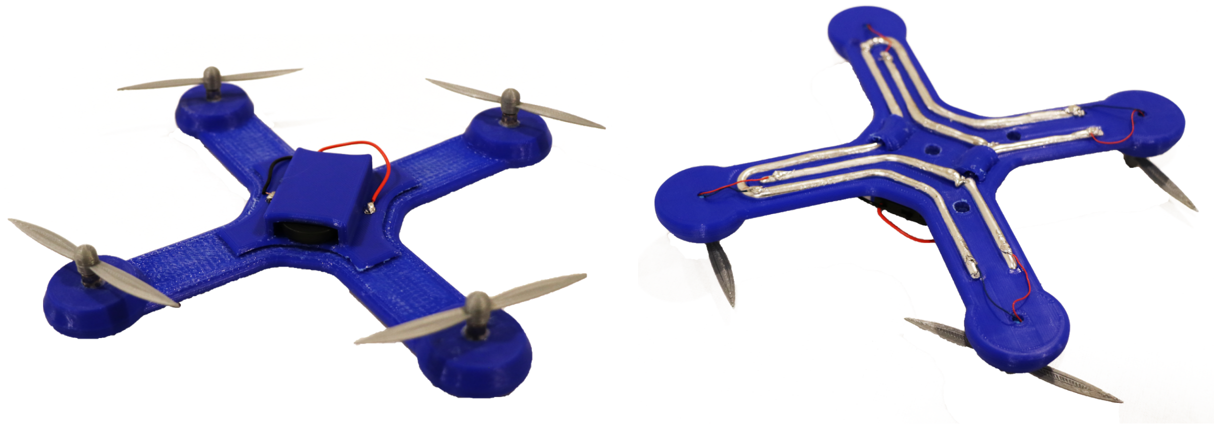

Figure 20: Printed Drone Totem, Isometric Top View (left) and Isometric View of Channels (right)

5.3. Achieving Stakeholder Benchmarks

Ultimately, five of the six original stakeholder benchmarks for the project were successfully achieved. The calculated fixed system cost was $715, below the $750 metric set from stakeholder research. A simplified breakdown of these costs can be found in **Appendix A9.** The resistance of the resulting traces was found to be 0.06 Ω, lower than the benchmark 0.25 Ω by a significant margin. Calculations leading to this resistance compared to the expected resistance can be found in **Appendix A3**, which further explains how this discrepancy and apparent improved performance came about.

Most importantly, Trace3D was able to successfully demonstrate printing ability in all three dimensions by demonstrating a complete, arbitrary 2D solder printing profile as well as by stacking solder droplets through vias built into the drone totem. The average build speed for creating the drone totem on the Trace3D system was 59 in/min. This was calculated by taking a weighted average of the speeds and associated times it took to complete both plastic and solder deposition. The post-processing time for the drone totem was only 10 minutes, which was lower than the expected 15 minutes. Post-processing for this specific print involved removing supports from the plastic body, installing and quickly connecting the leads from the outboard motors to the conductive traces, and connecting the battery pack to the printed circuitry through the internal vias.

The only benchmark that was not met was that relating to the variable material cost. Stakeholders seemed to indicate that they would be okay with a material cost of up to around $65/kg, but the raw cost of the solder wire and plastic filament used for this project came out to be $92/kg. This discrepancy can largely be attributed to the fact that relatively few suppliers are selling the solid core solder wire that was ultimately used for the drone totem in retail-size quantities. Additionally, more solder wire than would otherwise be needed had to be used in this print due to limitations with the off-the-shelf nozzle options. The team is confident that, in the future, if material were to be purchased at scale that this variable material cost metric for the user would be reduced significantly.

6. Conclusions and Future Work

In summary, Trace3D demonstrated a proof-of-concept system for an electromechanical 3D printer that uses off-the-shelf materials to create physical prototypes that integrate insulative structural components and conductive pathways in three dimensions. This was done using a highly retrofitted Ender 3 Pro 3D printer to extrude solder wire onto a plastic wafer in three dimensions. The representative test totem print was a drone where all conductive connections were made through the deposited solder wire itself. Key efforts related to this proof-of-concept included extensive stakeholder outreach, component and material selection, the design and manufacturing of a 1D gantry and all associated validation testing, quantitative analysis of the solder extrusion process, development of a slicer for custom G-Code generation, and finally the modification of the Ender 3 Pro to implement the solution in three dimensions. The team met five of the six stakeholder benchmarks for the Trace3D prototype, and anticipates being able to meet the sixth benchmark once at scale.

With this proof-of-concept, the team was only able to replace the wires that would otherwise be present in the drone - not the circuit board entirely. This was primarily due to limitations placed on the trace size that was printable by the off-the-shelf components that were selected. A smaller nozzle aperture size could be used in the future to make these traces smaller, as drop radius (and hence trace size) is a function of nozzle aperture. The team experimented with aperture sizes smaller than 0.6mm but was unable to make them work after running into issues with the solder pooling up and leaking out of the top of the nozzle shank between prints. Future work in this area would include designing our own nozzle with a longer bimetallic entrance shank, which would enable the extruder system to avoid leakage typical of smaller apertures when new solder wires are introduced by keeping the solder wire solid until far lower in the nozzle. Furthermore, a second heating cartridge could be added to the hotend to allow for solder deposition at a higher flow rate without temperatures dropping at the nozzle. With such a nozzle installed, significantly smaller traces could be printed and Trace3D can move towards printing full circuits.

Another key piece of future work needed to reach the capability to print full circuits and eventually entirely three dimensional, distributed printed circuit boards is integrating pick-and-place capability. This would involve a miniature robotic arm or vacuum-gripping system that could automatically place surface-mounted electronic components needed for any given circuit into the plastic matrix of the print when needed. Then, the conductive filament would connect all these components together. Finally, more solder alloys should certainly be explored in greater depth in future studies and projects in order to ensure that the absolute most optimal alloy is in use with the system.

With smaller trace sizes, a completely optimized material selection, and integrated pick-and-place capabilities, we believe that Trace3D can realize our broader vision of increased design freedom, more capability and creativity, and simplified development cycles for hobbyist and professional makers.

7. Statement of Roles

7.1. John Berg

John worked across many aspects of the project. Some of his major thrusts included stakeholder surveys, downselection and component research and selection, solder deposition and flow regime calculations, and creation of a MATLAB script for custom G-code generation for solder deposition in simple 2D shapes. He also secured sponsorships for the team and completed various supplementary CAD tasks for the test gantry, final system form CAD, and retrofitted Ender 3 Pro. He further contributed to all team presentations and other team deliverables.

7.2. Kevin Chazotte

Kevin had a significant role on the team, contributing to every component of the project that involved making things move and bringing them to reality. He led the team's mathematical analysis, literature review, and research analysis and contributed to early design work. After starting to work on electromechanical systems, he was responsible for the team's electronics development and software writing, including development of custom electronics and software for the test gantry, editing of G-Code scripts in MATLAB, development of two Java programs for implementing G-Code, and running G-Code over Octoprint. He further led all of the testing sessions with the retrofitted printer and contributed largely to testing on the test gantry.

7.3. Owen Ford

Owen was responsible for the design of the 1D test gantry, CAD for the future vision of the final system form, as well as several other smaller CAD tasks such as those related to the modification of the Ender 3 Pro. He worked closely with SEN3D as he constructed the 3D implementation gantry and was present to provide technical support and debugging help for it throughout every testing session.

7.4. Aviva Hurvitz

Aviva worked heavily on the design of the overall project, focusing on pitch deck creation and design, as well as photo and video content creation and editing for the final presentation. She also worked on various other aspects of the project, such as some CAD and fabrication, extensive stakeholder research, solder deposition calculations, and full documentation of the product and the process. She was also in charge of purchasing requests and communication with the university.

7.5. Jared Rogers

Jared primarily worked as Trace3D's project manager, which involved setting team goals and timelines, monitoring progress and status on all deliverables, and managing most team logistics. He drove most major team decisions and participated in all aspects of design, manufacturing, and validation of the Trace3D system. He generously hosted all Senior Design build and test sessions in his apartment, supported all other team members with their roles, and led all major presentation and writeup thrusts.

8. Acknowledgements

We'd like to acknowledge the following individuals for their contributions to this project:

- Kevin Turner, professor in Mechanical Engineering and Applied Mechanics (MEAM) at the University of Pennsylvania (Penn), for providing the team both with his recommendations for how to proceed with the project and his expertise on materials, specifically relating to wettability - a crucial aspect of our project's success
- Paulo Arratia, professor in MEAM at Penn, for providing guidance on the study of droplet deposition and how that related to printing with solder
- Peter Bruno, educational laboratory coordinator in MEAM at Penn, and the whole MEAM labs staff, for their consultation on manufacturing
- Graham Wabiszewski, senior lecturer in MEAM at Penn, our Senior Design teaching assistants Pranav Garg and Javier Becerra, and the entire Senior Design teaching staff for their support and assistance throughout the project

We would also like to thank our sponsors:

- Performance 3-d (P3-d) for their generosity in providing the team with a set of aluminum 3D printer nozzles with varying apertures
- Hillock Anodizing, for anodizing our aluminum nozzles on two different occasions over the year and for giving the team a tour of their facility
- Indium Corporation, for providing the team with unique solder alloys to test
- SEN3D and founder Kane Powley, for working closely with the team as we worked to retrofit the Ender 3 Pro with a second independent extruder head

This project would not have been possible without the generosity of these people and companies with their time, expertise, and supplies.

9. References

[1] Bot Factory, "Bot Factory SV2," Bot Factory [Online]. Available: https://www.botfactory.co/ [Accessed: 5-Dec-2020].

[2] Voltera, "Voltera V-One," *Voltera*. [Online]. Available: https://www.voltera.io/store/v-one. [Accessed: 23-Oct-2020].

[3] "Prometheus PCB Milling Machine," *Zippy Robotics, Inc*. [Online]. Available: https://shop.zippyrobotics.com/products/prometheus-pcb-milling-machine. [Accessed: 23-Oct-2020].

[4] "Desktop CNC: Bantam Tools Desktop PCB Milling Machine," *Bantam Tools*. [Online]. Available: https://www.bantamtools.com/pcb-milling-machine. [Accessed: 28-Oct-2020].

[5] "Printed Circuit Board Assembly: Circuit Card Assemblies: NEO Tech," *NEOTech*, 27-Jan-2020. [Online]. Available: https://www.neotech.com/manufacturing-services/pcba/. [Accessed: 09-Dec-2020].

[6] "3D Printed Electronics - Aerosol Jet Technology ," *Optomec*, 02-Aug-2018. [Online]. Available: https://optomec.com/printed-electronics/aerosol-jet-technology/. [Accessed: 23-Oct-2020].

[7] N.D.U.S.A. Inc., "DragonFly LDM System," *Nano Dimension*. [Online]. Available: https://www.nano-di.com/ame-dragonfly-ldm. [Accessed: 23-Oct-2020].

[8] M. Molitch-Hou, "Voxel8: 1st Electronics 3D Printer," *3D Printing Industry*, 05-Jan-2015. [Online]. Available: https://3dprintingindustry.com/news/voxel8-unleashes-electronics-3d-printer-ces-world-39060/. [Accessed: 23-Oct-2020].

[9] M. Molitch-Hou, "Voxel8 Returns to 3D Print Shoe Uppers," *Engineering.com*, 19-Nov-2019 [Online]. Available: https://www.engineering.com/3DPrinting/3DPrintingArticles/ArticleID/19735/Voxel8-Returns-to-3D-Print-Shoe-Uppers.aspx. [Accessed: 23-Oct-2020].

[10] "Standard Silver Ink (3 cc) (5 Units)," *Voxel8*. [Online]. Available: http://store.voxel8.com/product-catalog/standard-silver-ink-3-cc. [Accessed: 22-Oct-2020].

[11] Moorefield-Lang et. al, "Makerspaces in the high school setting: the student perspective." *Qualitative and Quantitative Methods in Libraries (QQML) Special Issue School Library Research and Educational Resources*, 13-Apr-2017. [Online]. Available: https://libres.uncg.edu/ir/uncg/f/H_Moorefield_Lang_Makerspaces_2019.pdf [Accessed: 03-May-2021]

[12] Rainwater, B. "How Cities Can Grow, The Maker Movement." *nlc.org,* 2016. [Online]. Available: https://www.nlc.org/wp-content/uploads/2016/12/Maker-Movement-Report-final.pdf [Accessed: 01-May-2021

[13] "Global Printed Circuit Boards (PCBs) Industry." *GlobeNewswire News Room*, 22-Aug-2020. [Online]. Available:

www.globenewswire.com/news-release/2020/08/22/2082261/0/en/Global-Printed-Circuit-Boards-PCBs-Industry.html [Accessed: 01-May-2021]

[14] Gaille, Brandon. "14 Printed Circuit Board Industry Statistics, Trends & Analysis." *BrandonGaille.com*, 18-Sept-2018. [Online]. Available: https://brandongaille.com/14-printed-circuit-board-industry-statistics-trends-analysis/ [Accessed: 03-May-2021]

[15] Liu, Huan, et al. "Emissions and Health Impacts from Global Shipping Embodied in US–China Bilateral Trade." *Nature News*, 28-Oct-2019. [Online]. Available: www.nature.com/articles/s41893-019-0414-z [Accessed: 01-May-2021]

[16] N. Mobsby, "Ender 3 Cura Settings: The Best Ender 3 Cura Profile," *All3DP*, 25-Sep-2020. [Online]. Available: https://all3dp.com/2/ender-3-cura-settings-best-ender-3-cura-profile/. [Accessed: 22-Oct-2020].

[17] "Bringing Functional Materials to 3D Printing," *Printed Electronics World*. [Online]. Available: https://www.printedelectronicsworld.com/articles/7637/bringing-functional-materials-to-3d-printing. [Accessed: 22-Oct-2020].

[18] MatterHackers, "White MH Build Series PLA Filament - 1.75mm (1kg)," *MatterHackers*. [Online]. Available: https://www.matterhackers.com/store/l/175mm-pla-filament-white-1-kg/sk/MEEDKTKU?rcode=GAT9HR&gclid=Cj0KCQjwufn8BRCwARIsAKzP696diBx2mpPo3ghkShzelcS3LRP4Zh2QfXeZXVZvxrH3lhNPrUl6Ro0aArCFEALw_wcB. [Accessed: 22-Oct-2020].

[19] Additive manufacturing - General principles - Terminology, ISO/ASTM 52900, 2015

[20] Standard Terminology for Additive Manufacturing Technologies, ASTM F2792, 2012

[21] Standard terminology for additive manufacturing - Coordinate systems and test methodologies, ISO/ASTM 52921, 2013

[22] Standard Guide for Evaluating Mechanical Properties of Metal Materials Made via Additive Manufacturing Processes, ASTM F3122, 2014

[23] Requirements for Printed Electronics Base Materials (Substrates), IPC-4921A, 2017

[24] Requirements for Printed Electronics Functional Conductive Materials, IPC-4591A, 2018

[25] Standard Specification for Solder Metal, ASTM B32-08, 2012

[26] Requirements For Electronic Grade Solder Alloys And Fluxed And Non-Fluxed Solid Solders For Electronic Soldering Applications, IPC J-STD-006B, 2006

[27] Kester, "Leaded Solid Solder Wire for High Reliability Soldering." *Kester.* [Online]. Available: https://www.kester.com/DesktopModules/Bring2mind/DMX/Download.aspx?Command=Core_Download&EntryId=1143&language=en-US&PortalId=0&TabId=96. [Accessed: 13-Apr-2021].

[28] "Solder Wire Price Per Kg Solder Wire Price Per Kg China," *Alibaba.com*. [Online]. Available: https://www.alibaba.com/showroom/solder-wire-price-per-kg.html. [Accessed: 22-Oct-2020].

[29] Y. S. Touloukian, *Thermophysical properties of matter: the TPRC data series; a comprehensive compilation of data by the Thermophysical Properties Research Center (TPRC), Purdue Univ.* New York: IFI, 1977.

[30] Tatsuta, “Functional Materials,” *TATSUTA Electric Wire & Cable Co., Ltd.* [Online]. Available: http://www.tatsuta.com/products/functional-material/paste/. [Accessed: 22-Oct-2020].

[31] “Voxel8 - The World's First 3D Electronics Printer,” *YouTube*, 24-May-2016. [Online]. Available: https://www.youtube.com/watch?v=adK5nGzAeWM. [Accessed: 21-Oct-2020].

[32] “Flexion HT,” *Diabase Engineering*. [Online]. Available: https://www.diabasemachines.com/product-page/flexion-ht. [Accessed: 08-Dec-2020].

[33] “Prometheus V2 Hot End,” *DisTech Automation.* [Online]. Available: https://www.distechautomation.com/products/prometheus-v2. [Accessed: 08-Dec-2020].

[34] “E3D Hemera Direct Kit (1.75mm),” *E3D Online*. [Online]. Available: https://e3d-online.com/products/e3d-hemera-direct-kit-1-75mm. [Accessed: 08-Dec-2020].

[35] “E3D All-metal v6 HotEnd Fully Assembled - 1.75mm Universal (Direct) (24v),” *MatterHackers.* [Online]. Available: https://www.matterhackers.com/store/l/e3d-all-metal-v6-hotend-fully-assembled-1.75mm-universal-direct-24v/sk/MUZ58LEM. [Accessed: 08-Dec-2020].

[36] “The Mosquito® Hotend,” *Slice Engineering*. [Online]. Available: https://www.sliceengineering.com/collections/mosquito-the-professional-hotend/products/the-mosquito-hotend™. [Accessed: 08-Dec-2020].

[37] “E3D Titan Aero HotEnd and Extruder - 3.00mm (24v),” *MatterHackers*. [Online]. Available: https://www.matterhackers.com/store/l/e3d-titan-aero-extruder-24v-300mm/sk/MY7HTR2K. [Accessed: 08-Dec-2020].

[38] “Micro Swiss Direct Drive Extruder for Creality Ender 5 with Hotend,” *MatterHackers*. [Online]. Available: https://www.matterhackers.com/store/l/micro-swiss-direct-drive-extruder-for-creality-ender-5/sk/M3LCYRZ8. [Accessed: 08-Dec-2020].

[39] “SeeMeCNC EZR Struder Extruder Kit,” *MatterHackers*. [Online]. Available: https://www.matterhackers.com/store/l/seemecnc-ezrstruder-kit/sk/MWHJ83XV. [Accessed: 08-Dec-2020].

[40] “Bondtech BMG-M Extruder - 1.75mm,” *MatterHackers*. [Online]. Available: https://www.matterhackers.com/store/l/bondtech-bmg-m-175/sk/MD2887LE. [Accessed: 08-Dec-2020].

[41] “Vanadium™ Nozzle,” *Slice Engineering*. [Online]. Available: https://www.sliceengineering.com/collections/nozzles/products/vanadium-nozzle™. [Accessed: 08-Dec-2020].

[42] “Olsson Ruby Nozzle - High Temperature - 1.75mm x 0.80mm,” *MatterHackers*. [Online]. Available: https://www.matterhackers.com/store/l/olsson-ruby-nozzle-high-temperature-175-080/sk/MP0U6LJH. [Accessed: 09-Dec-2020].

[43] "V6 Nozzles," *E3D Online*. [Online]. Available: https://e3d-online.com/products/v6-nozzles?variant=33409241579579. [Accessed: 09-Dec-2020].

[44] "Duraplat3-d™ Extruder Nozzles," *p3-d*. [Online]. Available: https://www.p3-d.com/collections/duraplat-3d-extruder-nozzles. [Accessed: 09-Dec-2020].

[45] M. Song, K. Kartawira, K. D. Hillaire, C. Li, C. B. Eaker, A. Kiani, K. E. Daniels, and M. D. Dickey, "Overcoming Rayleigh–Plateau instabilities: Stabilizing and destabilizing liquid-metal streams via electrochemical oxidation," Proceedings of the National Academy of Sciences, vol. 117, no. 32, pp. 19026–19032, Jul. 2020.

[46] 60-40 Soft Solder (60 Sn-40Pb) - ASTM B 32 Grade Sn60. [Online]. Available: http://www.matweb.com/search/datasheet_print.aspx?matguid=06a31d97bb734b509043d81cf131b280. [Accessed: 01-Mar-2021].

[47] T. L. Bergman, A. Lavine, and F. P. Incropera, *Fundamentals of heat and mass transfer*. Hoboken, NJ: John Wiley & Sons, Inc., 2019. [Accessed: 01-Mar-2021]

[48] "PCB Trace Width Calculator," *Porto*. [Online]. Available: https://www.7pcb.com/trace-width-calculator.php. [Accessed: 01-Mar-2021]

[49] "Printed Circuit Board Prototype," *Custom PCB Prototype Manufacturer*. [Online]. Available: https://www.pcbway.com/pcb_prototype/Pinted_Circuit_Board_Prototype.html. [Accessed: 01-Mar-2021]

[50] "PCB Capabilities," *JLCPCB*. [Online]. Available: https://jlcpcb.com/capabilities/Capabilities. [Accessed: 01-Mar-2021]

[51] Multicore Solders, "Properties of Solder" 315929 datasheet

[52] SD3D, "PLA Technical Data Sheet" MaterialTDS-PLA_01 datasheet, June 2017.

[53] "Gcode dictionary," Duet3D. [Online]. Available: https://duet3d.dozuki.com/Wiki/Gcode. [Accessed: 01-May-2021]

Appendix

A1: Competitive Landscape 2x2 Comparison

Comparing all competitive offerings on a grid comparing price and dimensionality, it is apparent that Trace3D occupies a unique position as an affordable 3D option.

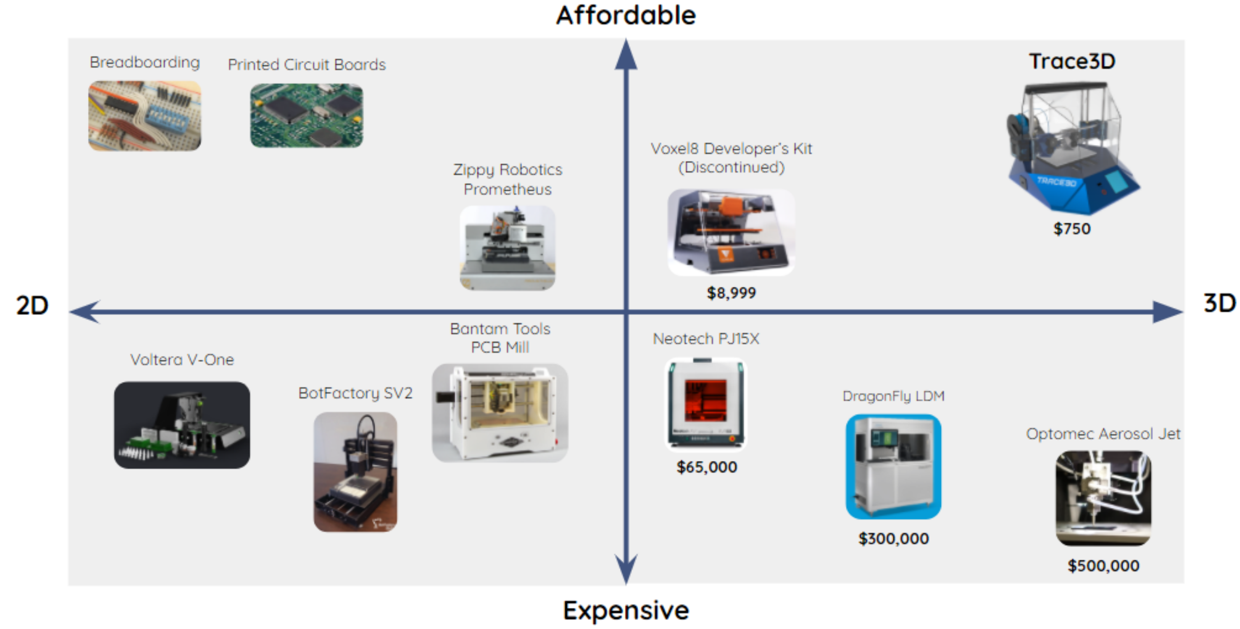

Similarly, based on target market and speed, Trace3D once again occupies a niche position as a relatively fast machine that is meant for prototyping components.

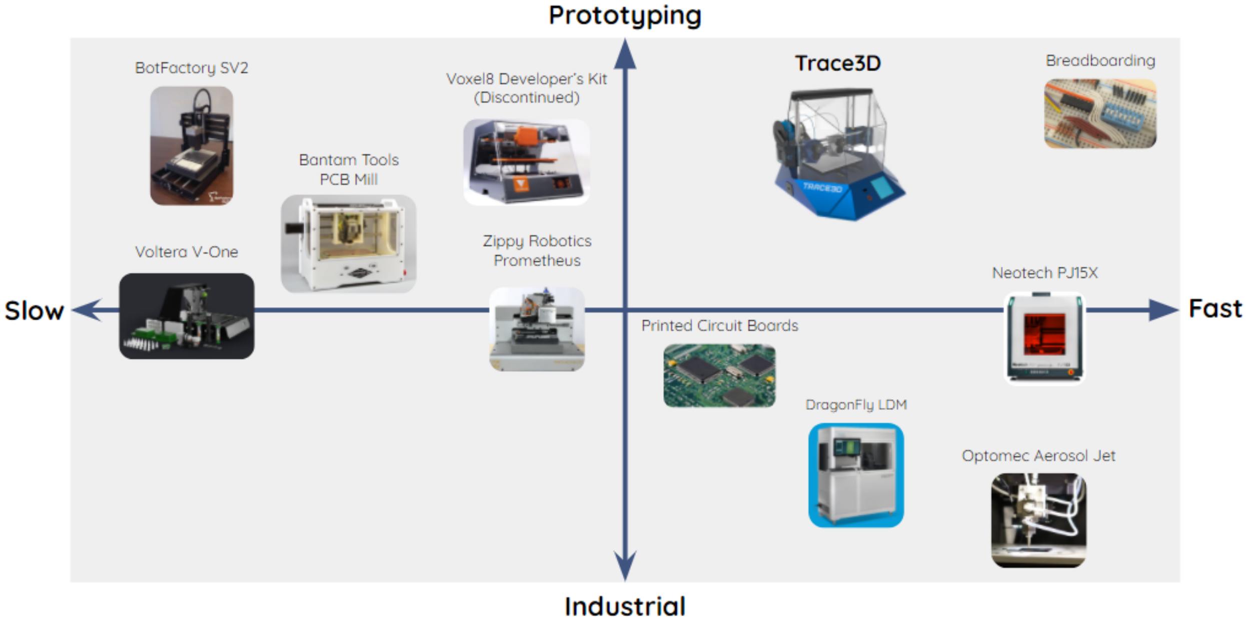

A2: Quadcopter Development

What follows is a visualization of the Trace3D simplified assembly process with the quadcopter example. Without Trace3D, as seen on the left, you would start with your mechanical chassis, install the control chip and motors in place, fasten it together, and then frustratingly connect wires from the inboard PCB to the outboard motors. With Trace3D, half the chassis is 3D printed, the control board is placed and embedded inside, traces are printed internally connecting to the motor, and finally some surface mounted components are added last.

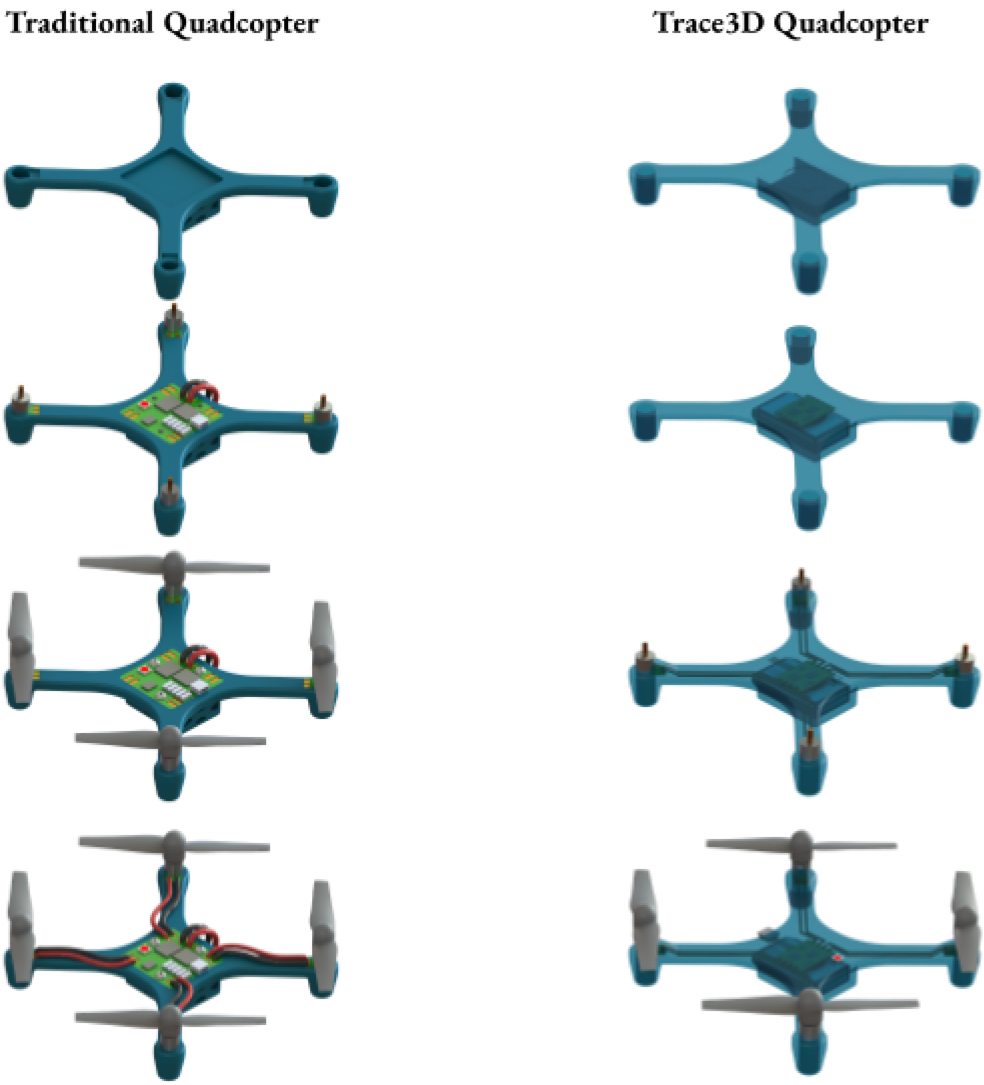

A3: Resistivity of Solder Traces

The electrical resistance of a trace is calculated as follows:

$$R = \frac{\rho l}{tw} \text{ x } (1 + \alpha \text{ x } (T_{\text{ambient}} - 25°\text{C})),$$

For a typical copper trace with 1 oz copper (or 0.036 mm) thickness [48, 49, 50], 0.127 mm line width [48, 49, 50], electrical resistivity $\rho = 1.68 \text{ x } 10^{-8}\Omega\text{m}$ [29], resistive temperature coefficient $\alpha = 0.00404 \text{ K}^{-1}$ [29], 65 mm length, and $T_{\text{ambient}} = 40$ °C, we can show that the resistance will be:

$$\begin{aligned} R &= \frac{\rho l}{tw} \text{ x } (1 + \alpha \text{ x } (T_{\text{ambient}} - 25°\text{C})) \\ R &= \frac{1.68 \text{ x } 10^{-8}\Omega\text{m x } 65\text{mm}}{0.127\text{mm x } 0.036\text{mm}} \text{ x } (1 + 0.00404 \text{ K}^{-1}\text{x } (40°\text{C} - 25°\text{C})) \\ R &= 0.253\Omega \end{aligned}$$

or, 0.253 Ohms for this representative trace.

For a typical solder trace with 0.107 mm thickness, 0.381 mm line width, electrical resistivity $\rho = 14.5 \text{ x } 10^{-8}\Omega\text{m}$ [29], resistive temperature coefficient $\alpha = 0.00612 \text{ K}^{-1}$ [29], 65 mm length, and $T_{\text{ambient}} = 40$ °C, we can show that the resistance will be:

$$\begin{aligned} R &= \frac{\rho l}{tw} \text{ x } (1 + \alpha \text{ x } (T_{\text{ambient}} - 25°\text{C})) \\ R &= \frac{14.5 \text{ x } 10^{-8}\Omega\text{m x } 65\text{mm}}{0.381\text{mm x } 0.107\text{mm}} \text{ x } (1 + 0.00612 \text{ K}^{-1}\text{x } (40°\text{C} - 25°\text{C})) \\ R &= 0.252\Omega \end{aligned}$$

or, 0.252 Ohms for this representative trace, just lower than that of the copper trace. In our validation, we attempted to show proof of concept results with resistances less than or equal to this calculated resistance for a 65-mm trace, while varying the geometries of the trace to suit our purposes.

Material	Trace Length (mm)	Width (mm)	Thickness (mm)	T_{amb} (°C)	Resistance (Ω)
Copper Trace	65	0.127	0.036	40	0.253
Solder Wire	65	0.381	0.107	40	0.252

From stakeholder research about users' expectations for Trace3D, it was evidently important to maintain resistance values similar to those of copper traces in a PCB to avoid unwanted voltage drops. We set our resistance metric by acknowledging that we could print a solder trace larger and thicker than that of a copper trace and, in so doing, keep the same effective resistance despite the solder's resistivity being larger. This relationship can be shown in the above calculations, where we triple the width and thickness of the printed solder traces to maintain a lower resistance than that of the copper trace.

The team selected a typical trace length that may be present on any kind of consumer electronic printed circuit board of roughly 2.5 inches. For that length, the expected resistance of a copper trace, with thicknesses and widths determined by PCB manufacturers [48, 49, 50], comes out to 0.253 Ω. As mentioned above, the solder traces we propose outperform this resistance by using increased length and width to reach a calculated resistance of 0.252 Ω. In order to qualify our stakeholder needs during testing, we designed our 1D test coupons to be roughly 2.5 inches in length so that we could quickly and easily check resistance values against this benchmark.

We were able to experimentally determine resistances in the extruded traces by simply measuring across them with a high-precision digital multimeter. These measurements showed that our printed traces, while larger in size than the traces discussed in the above calculations, demonstrated a far lower resistance. Indeed, the measured resistance with our digital multimeter was 0.06 Ω, almost an order of magnitude lower than our target. However, re-performing the above calculations with the channel geometry that we used for this metric found that the theoretical value could have been 0.006 Ω, another order of magnitude difference. We attribute the difference between our experimental results and theoretical calculations to oxide layers formed during the printing process, which was a factor that we were concerned about during our testing and aimed to minimize in our final results.

A4: Solder Deposition

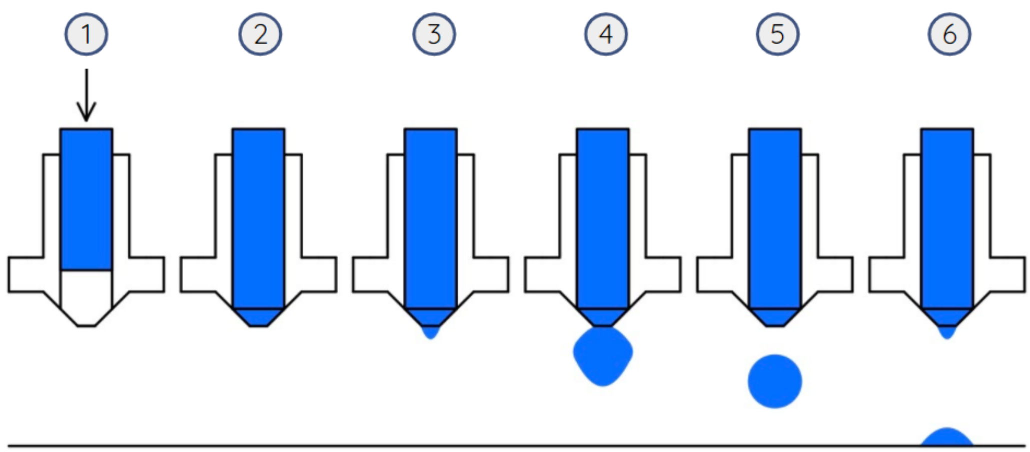

Solder deposition works as follows: first the solder wire is forced into the hotend where it is melted and begins to form a drop on the tip of the nozzle. Once the drop is big enough, it falls, and a new drop begins to form. This is repeated until a full trace is formed, at which point the wire is driven out.

A5: Circuit Diagram & Soldered Perf Boards

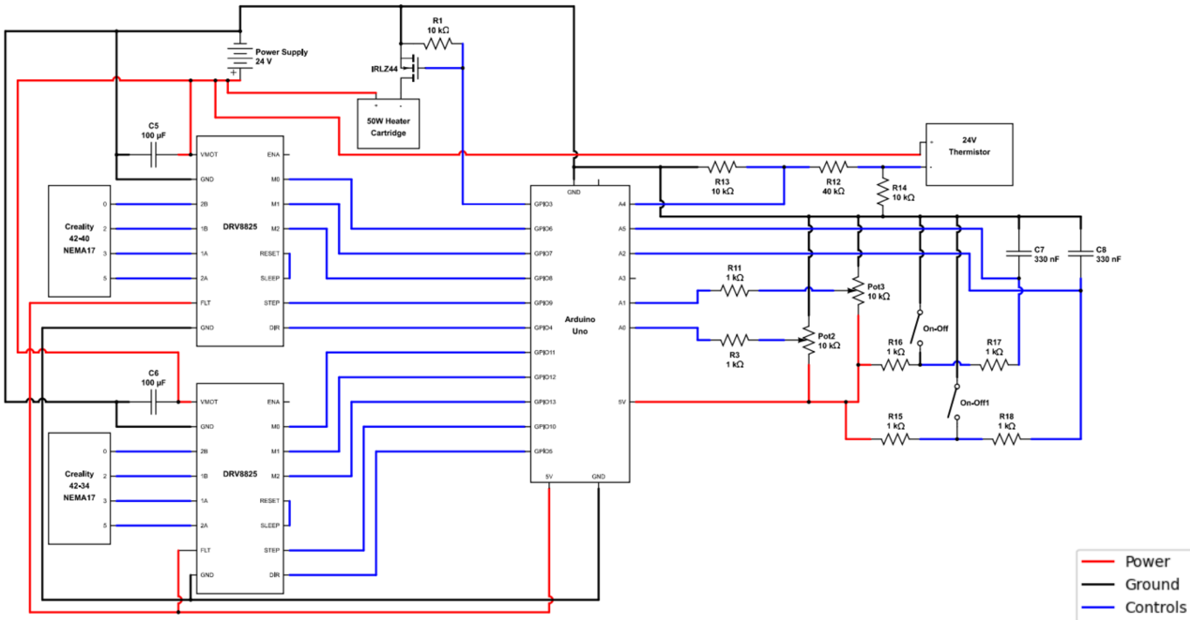

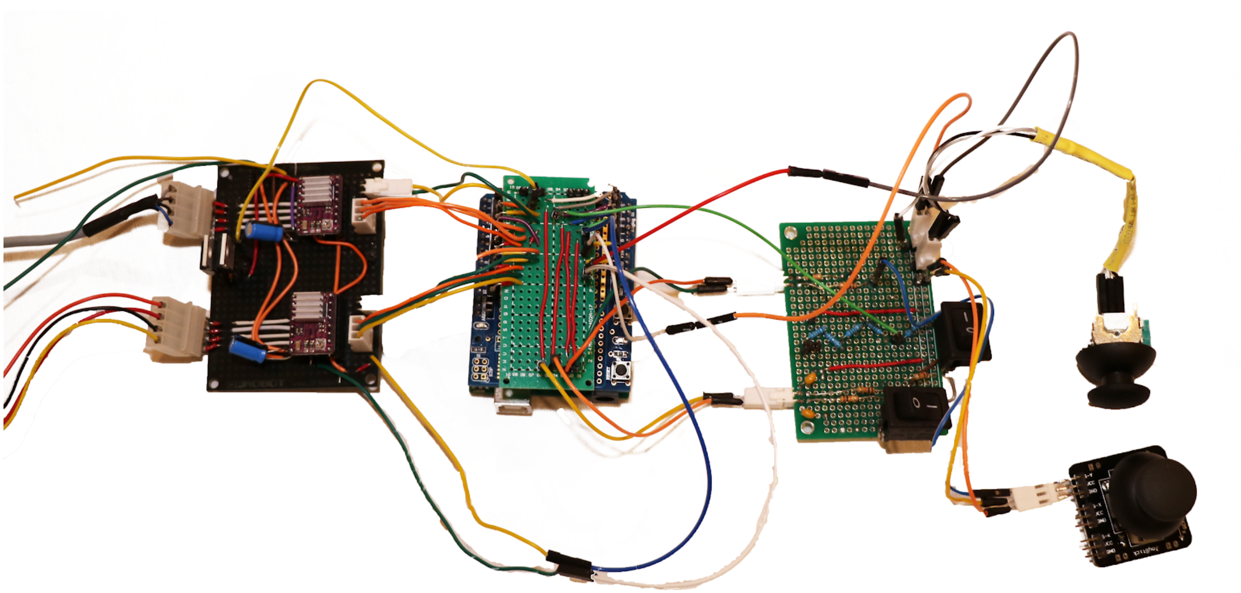

A6: Experimental Data from 1D Test Gantry Testing

The first proof-of-concept testing began with very small nozzle heights and with nozzle apertures of 0.4 mm or 0.8 mm in size. Notably, these tests were good for proof-of-concept results, but the actual printed traces were very poor. Most of them did not have continuity, nor did they have very good adhesion to the plastic.

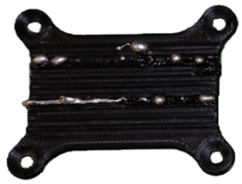
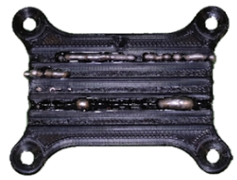
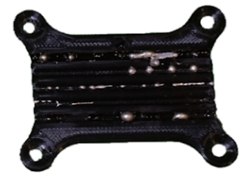

Testing Parameter	Test Coupon #0	Test Coupon #1	Test Coupon #2
Nozzle Aperture	0.8 mm	0.4 mm	0.4 mm
Nozzle Height	0.036 in	0.021 in	0.034 in
Channel Radius	0.035 in	0.05 in	0.0375 in
Feed Rate	5.81 in/min	5.81 in/min	5.81 in/min
Results	Horrible continuity	Barely any adhesion	Nozzle clogged

We then began increasing the nozzle height significantly and also switched out the nozzle aperture for two of the next prints. Test coupons three and five, shown here, had great adhesion and generated well-developed traces with very low resistance.

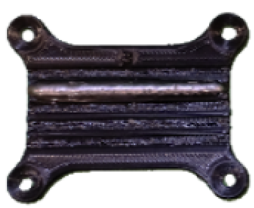
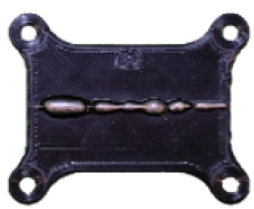
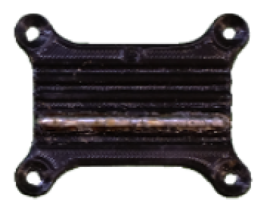

Testing Parameter	Test Coupon #3	Test Coupon #4	Test Coupon #5
Nozzle Aperture	0.6 mm	0.4 mm	0.6 mm
Nozzle Height	0.145 in	0.036 in	0.132 in
Channel Radius	0.075 in	0 in	0.05 in
Feed Rate	8.53 in/min	8.53 in/min	8.53 in/min
Results	Fantastic, great adhesion	Decent, gaps in trace	Good, but worse adhesion

A7: Drone Totem Iterations

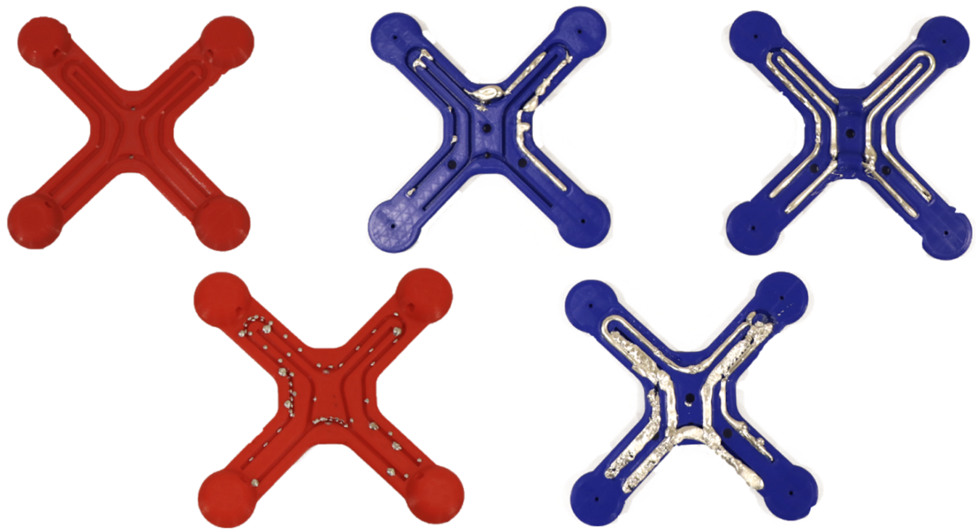

A8: Pictures of Successful Drone Totem Print

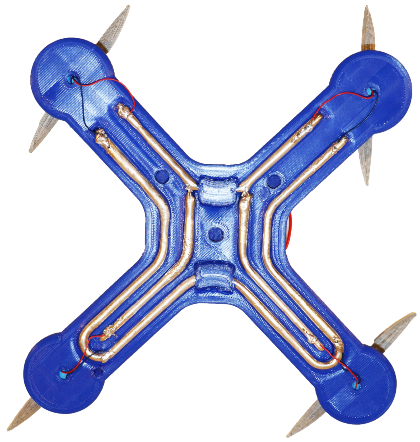

A9: Fixed Cost Breakdown

Table 6: Simplified Trace3D Fixed Cost Breakdown

Expense	Cost	Notes
Ender 3 Pro	$205	The printer the team retrofitted
Hotend & Cooling Subsystem	$155	All hotend and cooling parts
Extruder & Nozzle Subsystem	$90	The entire extrusion assembly
Second Extruder Parts	$265	Everything needed to add extruder head #2
Total	$715	